

Robust Design of Multi-cell D2D Communication under Partial CSI

Ali Ramezani-Kebrya, *Member, IEEE*, Ben Liang, *Fellow, IEEE*, Min Dong, *Senior Member, IEEE*,
and Gary Boudreau, *Senior Member, IEEE*

Abstract—We consider device-to-device (D2D) communication underlaid in a cellular network to share the uplink resource of cellular users (CUs). It is a key technology in the emerging Internet of Things to support vehicle-to-everything communication networks. In a multi-cell scenario, both D2D pairs and CUs may cause significant inter-cell interference (ICI) to the neighboring cells. Furthermore, due to substantial signaling overhead, we assume only partial CSI of D2D links at the BS. We consider joint power control, beamforming, and CU-D2D matching problem, assuming partial CSI from D2D pairs under the general Nakagami fading model. We formulate a joint receive beamforming and robust power control optimization problem for a CU-D2D pair to maximize their expected sum rate under the power budget, while meeting the minimum SINR requirements and worst-case ICI limits at neighboring cells in probabilistic sense. We propose an efficient algorithm that combines an iterative D2D feasibility check and a ratio-of-expectation approximation. A performance upper bound is also developed for benchmarking. For multiple CUs and D2D pairs, due to orthogonal channelization within each cell, we first focus on the problem of joint power control and beamforming for a CU-D2D pair and show how our proposed solution can be leveraged to find a solution for this general problem. The complexity analysis of the proposed approach is also provided. Simulation results show that the proposed algorithm gives performance close to the upper bound.

Index Terms—Device-to-device communication, partial CSI, vehicle-to-everything, inter-cell interference, power control.

I. INTRODUCTION

Intelligent transportation and autonomous driving are among key services in the emerging world of Internet of Things (IoT). As an important application of IoT, vehicle-to-everything (V2X) communication networks establish smart, safe, and scalable vehicular communication to the cellular network, other vehicles, and pedestrians [2], [3]. The plethora of sensors deployed in the IoT ecosystem facilitate the collection, processing, and sharing of massive amount of data among vehicles, which is critical to sensitive applications such as autonomous driving [4]–[6]. In order to improve reliability and safety of intelligent transportation systems and reducing

traffic congestion, device-to-device (D2D) communication has been considered as a key technology to support V2X communication networks, where nearby users, *e.g.*, vehicles, can establish a direct communication link to transmit data to each other without going through the backhaul network [7]. D2D communication can improve the overall network utilization due to resource reuse by both the cellular users (CUs) and the D2D pairs [8]. In D2D-based V2X communication, due to substantial signaling overhead, full channel state information (CSI) of the D2D links and links between CUs and D2D pairs are not available at the base station (BS).

For D2D communication underlaid in a cellular system to reuse spectrum resource assigned to CUs, uplink resource sharing is attractive due to the low-cost receive chain requirement at the D2D receiver, a lighter traffic pattern than that of downlink, and the simplicity of interference management at the BS [8]. When a D2D pair reuses the channel resource of a CU, it causes intra-cell interference to the CU, and vice versa. Furthermore, its transmission generates inter-cell interference (ICI) to neighboring cells. To meet the SINR requirements of CUs and D2D pairs and to control the ICI to neighboring cells, D2D communication and its resource allocation scheme should be carefully designed and optimized.

Without the ICI consideration, intra-cell interference management among D2D pairs and CUs in a single-cell scenario has been studied extensively in the literature [9]–[18]. However, in practical scenarios, the ICI caused by both D2D pairs and CUs to neighboring cells often cannot be ignored. In particular, as the number of vehicles and IoT devices increases, ICI management is expected to become a prominent challenge to meet the requirements in future wireless systems. Furthermore, a vast majority of the existing literature on D2D-based V2X communication focus on resource allocation assuming full CSI of the D2D links and links between CUs and D2D pairs is available at the BS [9]–[26]. However, this ideal assumption imposes substantial signaling overhead for CSI feedback to the BS. In practical scenarios, the BS may not have full CSI knowledge of these links related to D2D pairs.

To address these challenges, in this paper, we consider a multi-cell uplink transmission scenario, where both the CUs and D2D pairs may cause significant ICI at multiple neighboring BSs. Furthermore, unlike many existing works that assume the BS with a single antenna for simplification, we study the case where the BS is equipped with multiple antennas, which is anticipated to be typical for 5G and beyond. We assume that only partial CSI is available at the BS. Since channels from the CU to the BS and from the D2D transmitter

This work was supported in part by Ericsson Canada, the Natural Science and Engineering Research Council (NSERC) of Canada, and an NSERC Postdoctoral Fellowship.

A. Ramezani-Kebrya is with EPFL, 1015 Lausanne, VD, Switzerland (e-mail: ali.ramezani@epfl.ch). B. Liang is with the Department of Electrical and Computer Engineering, University of Toronto, Toronto, ON M5S 1A1, Canada (e-mail: liang@comm.utoronto.ca). M. Dong is with the Department of Electrical, Computer and Software Engineering, Ontario Tech University, Oshawa, ON L1G 0C5, Canada (e-mail: min.dong@ontariotechu.ca). G. Boudreau is with Ericsson, Ottawa, ON K2K 2V6, Canada (e-mail: gary.boudreau@ericsson.com). Part of this work was presented in [1].

Copyright (c) 2021 IEEE. Personal use of this material is permitted. However, permission to use this material for any other purposes must be obtained from the IEEE by sending a request to pubs-permissions@ieee.org.

to the BS can be easily measured at the BS, they are assumed to be perfectly known. For all other channels, we assume only average channel gains are known at the BS. Under partial CSI, we formulate the joint receive beamforming and power control as a robust optimization problem, with the goal to maximize the expected sum rate of CUs and D2D pairs, under the probabilistic SINR target guarantees and the limit imposed on the expected worst-case ICI to other neighboring cells.

A. Main Contributions

- We consider the joint problem of power control, beamforming design, and CU-D2D matching in a multi-channel scenario with multiple D2D pairs and CUs under partial CSI with general Nakagami and Rayleigh fading models. This problem formulation leads to a difficult mixed integer program. We decompose this problem into a joint power optimization problem of a CU-D2D pair and a CU-D2D matching problem. We show how our power control solution for this problem can be leveraged to find a solution for the overall joint design for multiple CU-D2D pairs.
- Under optimal receive beamforming for the CU, we focus on the robust joint power control at one CU and one D2D transmitter for expected sum rate maximization. The formulated robust joint optimization problem is challenging to solve due to its non-convexity, and stochastic nature of the objective and constraints due to CSI uncertainty. We propose an efficient robust power control algorithm based on a ratio-of-expectation (ROE) approximation to maximize the expected sum rate. The robust power control solution of the CU and D2D is obtained by analyzing the feasible solution region of the problem and the characteristics of the solution in the feasible region. We then systematically find all candidates for the power control solution. An upper bound on the expected sum rate is developed to benchmark the performance of the proposed algorithm.
- Simulation shows that our proposed robust power control algorithm provides performance that is close to the upper bound we developed, and it substantially outperforms baseline algorithms. The analysis of the computational complexity of this approach is also provided.

B. Related Work

In underlay D2D-based V2X communication, power control and CU-D2D matching problems have been studied under full CSI [9]–[12], [23], [24]. Various schemes have been proposed in the literature to limit the intra-cell interference due to resource reuse by CUs and D2D pairs in a *single-cell* scenario under full CSI [13]–[22]. Since they do not consider the multi-cell setting, none of these works account for the ICI impact in the design. In contrast, in this paper, we consider ICI constraints and partial CSI, which is more realistic and important in practice, where ICI control and CSI acquisition are two main issues. Furthermore, unlike [9]–[24] in which a single-antenna BS is assumed, we consider a more typical scenario where each BS is equipped with multiple antennas.

In [25], [26], we have obtained an optimal power control solution for the sum rate maximization of a CU-D2D pair under a worst-case ICI limit to a neighboring cell, assuming full CSI. Different from [25], [26], in this paper, we focus on robust joint power control optimization of CU-D2D pairs with partial CSI.

D2D communication under partial CSI in a single cell has been studied in the literature. In [27], under the assumption of limited CSI at the users, the spectral efficiency and outage probability of a hybrid D2D system is analyzed by proposing a time-division uplink transmission scheme. With partial CSI knowledge of the interfering link from a CU to a D2D pair, probabilistic access control for the D2D pair has been proposed in [28] to maximize the expected sum rate for uplink resource sharing. In [29], centralized and distributed power control schemes are proposed to maximize the coverage probability under the assumption of imperfect CSI. Recently, in [12], a joint power control and resource allocation problem is studied to maximize the sum ergodic capacity of vehicular user equipments under imperfect CSI with consideration of Doppler effect due to the high mobility of vehicles in D2D-based V2X communication. However, none of [12], [27]–[29] consider the effect of ICI due to D2D communication in a multi-cell scenario, which is a prominent challenge in future wireless systems especially in the IoT environment. In a multi-cell scenario, the authors of [30] proposed a subchannel allocation scheme to assign D2D pairs to CUs under fixed transmit powers and partial CSI. Unlike [30], in this paper, we focus on robust power control problem.

There are certain similarities between resource management in cognitive radio systems and interference management in small cells with that of D2D systems. However, they bear different emphases that lead to different design formulations. The primary focus of cognitive radio literature is on the performance of secondary network, while we consider the overall performance of CU-D2D pairs. The power control techniques considered in [31] and references therein mainly involve transmit power optimization for small-cell users only rather than joint power control for both small-cell and macro-cell users. To the best of our knowledge, the joint design optimization problem considered in our paper has not been considered in the existing literature for small cells.

The rest of this paper is organized as follows. In Section II, the system model is described and the expected sum rate maximization problem is formulated. Section III presents the proposed algorithm to the expected sum rate maximization for one D2D pair and one CU. Then, the extension to multiple D2D pairs and CUs is presented in Section IV. Numerical results and complexity analysis are presented in Section V, followed by the conclusion in Section VI.

Notation: We use $\|\cdot\|$ to denote the Euclidean norm of a vector. \mathbf{I}_N stands for an $N \times N$ identity matrix. We use $\mathbf{a} \preceq \mathbf{b}$ to indicate that all entries of $\mathbf{b} - \mathbf{a}$ are non-negative.

II. SYSTEM MODEL AND PROBLEM FORMULATION

A. Cellular System with D2D Pairs

Consider a cellular system where the D2D pairs reuse the spectrum resource already assigned to the CUs for uplink

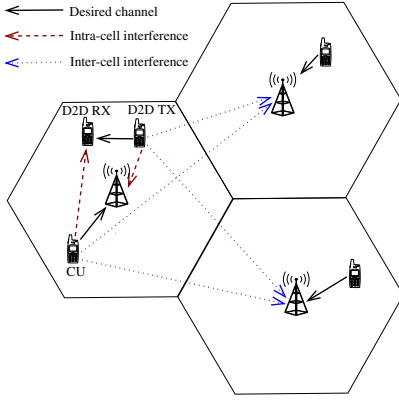


Fig. 1: The system model for uplink resource reuse.

communication. We assume that all users are equipped with a single antenna, and the BS is equipped with N antennas. The BS coordinates the transmission of the CU and D2D pair. We follow the conventional assumption of orthogonal spectrum resource allocation among CUs in a cell. Thus, these CUs do not interfere with each other. When a D2D pair communicates using the channel of a CU, they cause intra-cell interference to each other.

We consider a multichannel communication system (e.g., OFDMA) with N_C orthogonal subchannels in each cell. We assume a fully loaded network with N_C CUs and N_D D2D pairs per cell where each CU occupies one subchannel. Without loss of generality, we assume CU j uses subchannel j for $j \in \mathcal{C} \triangleq \{1, \dots, N_C\}$. Each D2D pair reuses at most one subchannel, and the subchannel of each CU can be reused by at most one D2D pair. Let $x_{k,j} \in \{0, 1\}$ indicate D2D pair k reuses CU j 's subchannel, i.e., $x_{k,j} = 1$ if D2D pair k reuses CU j 's subchannel; otherwise, $x_{k,j} = 0$.

B. SINR and ICI Expressions

Let $P_{D,k}$ and $P_{C,j}$ denote the transmit power of D2D pair k and CU j , respectively. Assume D2D pair k reuses CU j 's subchannel. The received signal at the BS on subchannel j is given by $\mathbf{y}_{C,j} = \sqrt{P_{C,j}}\mathbf{h}_{C,j}s_{C,j} + \sqrt{P_{D,k}}\mathbf{g}_{D,k}s_{D,k} + \mathbf{n}$, where $s_{C,j}$ and $s_{D,k}$ are the transmitted symbols from CU j and D2D k transmitters with $\mathbb{E}[|s_{C,j}|^2] = 1$ and $\mathbb{E}[|s_{D,k}|^2] = 1$, respectively, $\mathbf{h}_{C,j} \in \mathbb{C}^{N \times 1}$ is the channel between CU j and the BS, $\mathbf{g}_{D,k} \in \mathbb{C}^{N \times 1}$ is the interference channel between D2D k transmitter and the BS, and $\mathbf{n} \sim \mathcal{CN}(0, \sigma^2\mathbf{I})$. The uplink received SINR at the BS from CU j is given by

$$\gamma_{C,j} = \frac{P_{C,j}|\mathbf{w}_j^H \mathbf{h}_{C,j}|^2}{\sigma^2 + P_{D,k}|\mathbf{w}_j^H \mathbf{g}_{D,k}|^2} \quad (1)$$

where \mathbf{w}_j is the receive beam vector at the BS on subchannel j with unit norm, i.e., $\|\mathbf{w}_j\|^2 = 1$.¹ The received signal at D2D k receiver is given by $y_{D,k} = \sqrt{P_{D,k}}h_{D,k}s_{D,k} + \sqrt{P_{C,j}}g_{C,j}s_{C,j} + n_D$, where $h_{D,k} \in \mathbb{C}$ is the channel between D2D pair k , $g_{C,j} \in \mathbb{C}$ is the interference channel between CU

j and D2D k receiver, and $n_D \sim \mathcal{CN}(0, \sigma_D^2)$. The SINR at D2D k receiver is given by²

$$\gamma_{D,k} = \frac{P_{D,k}|h_{D,k}|^2}{\sigma_D^2 + P_{C,j}|g_{C,j}|^2}. \quad (2)$$

In a multi-cell network, both D2D and CU transmissions cause ICI in neighboring cells. In this work, we consider ICI for uplink transmission at b neighboring BSs. However, our approach can be applied also to ICI in a downlink scenario. Let $\mathbf{f}_{C,i,j} \in \mathbb{C}^{N \times 1}$ and $\mathbf{f}_{D,i,k} \in \mathbb{C}^{N \times 1}$ denote the ICI channels from CU j and D2D k transmitter to neighboring BS i , respectively, for $i = 1, \dots, b$. Since the beam vector at neighboring BS i is typically unknown to the CU and D2D pair, we consider the worst-case ICI on subchannel j given by³

$$P_{I,i,j} = P_{C,j}\|\mathbf{f}_{C,i,j}\|^2 + P_{D,k}\|\mathbf{f}_{D,i,k}\|^2. \quad (3)$$

Note that only channel power gains are needed to obtain $P_{I,i,j}$ in (3), i.e., instantaneous CSI is not required and CUs or D2D pairs do not need to know the receive beam vectors at neighboring BSs. Furthermore, we assume only $\mathbb{E}[\|\mathbf{f}_{D,i,k}\|^2]$ and $\mathbb{E}[\|\mathbf{f}_{C,i,j}\|^2]$ are available at the BS.

C. Partial CSI with General Distribution

We assume instantaneous CSI is available for $\mathbf{h}_{C,j}$ and $\mathbf{g}_{D,k}$, i.e., the direct channels from CU j and D2D k to the BS in Fig. 1. However, for $h_{D,k}$, $g_{C,j}$, $\{\mathbf{f}_{D,i,k}\}_{i=1}^b$, and $\{\mathbf{f}_{C,i,j}\}_{i=1}^b$, the BS knows only the distributions of these channels. We first assume a general Nakagami fading model for $h_{D,k}$ and $g_{C,j}$, where $|h_{D,k}|^2$ and $|g_{C,j}|^2$ follow Gamma distributions. Later, we focus our consideration to the special case of Rayleigh fading model. We assume the parameters in each channel distribution are known at the BS. Note that measuring and transmitting these statistical parameters is much easier than the instantaneous CSI [32].⁴ This substantially reduces the signaling overhead due to D2D communication. For the ICI channels, we assume only the interference channel power gain $\mathbb{E}[\|\mathbf{f}_{D,i,k}\|^2]$ and $\mathbb{E}[\|\mathbf{f}_{C,i,j}\|^2]$ are known at the BS scheduler.

D. Problem Formulation

Let P_C^{\max} and P_D^{\max} denote the maximum transmit power at the CU and D2D transmitters, respectively. Let $\mathbf{p} \triangleq [P_{D,1} \dots P_{D,N_D} P_{C,1} \dots P_{C,N_C}]^T$, $\mathbf{x} \triangleq [x_{1,1} \dots x_{1,N_C} \dots x_{N_D,1} \dots x_{N_D,N_C}]^T$, and $\tilde{\mathbf{w}} \triangleq [\tilde{\mathbf{w}}_1^T \dots \tilde{\mathbf{w}}_{N_C}^T]^T$.

²The terms σ^2 and σ_D^2 in (1) and (2) can be viewed as the receiver noise power plus the ICI power. In particular, since in this work we consider an ICI management scheme where the transmitters in each cell guarantee a worst-case ICI amount, we can use the upper bounds of ICI components as expressed in (3). Then, the CU rate expression $\log(1 + \gamma_C)$ is a lower bound on the capacity, and therefore, it is indeed achievable.

³Note that $P_{I,i,j}$ in (3) is an upper bound of the actual ICI. Let $\tilde{\mathbf{w}}_i$ denote the beam vector at neighboring BS i . If $\tilde{\mathbf{w}}_i$ is known, then we can consider the actual ICI through replacing $\|\mathbf{f}_{i,j}\|$ by $|\tilde{\mathbf{w}}_i^H \mathbf{f}_{i,j}|$ in (3).

⁴We define the overhead gain as the difference between the number of parameters required to be estimated under full CSI and that under partial CSI. Then, for a fully loaded network with N_C active CUs and N_D active D2D pairs, the overhead gain for this cell scales as $\Omega((N_D + N_C)bT)$ where T denotes the number of instantaneous CSI updates while the CSI statistics is fixed.

¹The norm of \mathbf{w} does not change the uplink SINR expression at the BS.

The expected sum rate maximization problem is formulated in this section. The objective is to maximize the overall expected sum rate of all D2D pairs and CUs by optimizing the transmit power vector \mathbf{p} , the D2D reuse indicator vector \mathbf{x} , and the receive beam vector $\hat{\mathbf{w}}$, while satisfying the worst-case ICI and SINR requirements under the per-node power constraints. Due to the partial CSI knowledge at each serving BS, the D2D SINR and ICI to each neighboring BS are unknown random variables. For the D2D pair's SINR requirement, we impose a constraint on the outage probability of meeting the SINR requirement. We also limit the expected worst-case ICI under a certain limit. The formulated problem is given by

$$\begin{aligned} \mathcal{R}_1 : \quad & \max_{(\mathbf{p}, \hat{\mathbf{w}}, \mathbf{x})} \sum_{k \in \mathcal{D}} \sum_{j \in \mathcal{C}} \log(1 + \gamma_{C,j}) + x_{k,j} \mathbb{E}[\log(1 + \gamma_{D,k})] \\ \text{subject to} \quad & \frac{P_{C,j} |\mathbf{w}_j^H \mathbf{h}_{C,j}|^2}{\sigma^2 + x_{k,j} P_{D,k} |\mathbf{w}_j^H \mathbf{g}_{D,k}|^2} \geq \gamma_C^{\min}, \quad \forall j \in \mathcal{C} \\ & \Pr\{\gamma_{D,k} \leq \gamma_D^{\min}\} \leq \epsilon, \quad \forall k \in \mathcal{D} \\ & \mathbb{E}[P_{I,i,j}] \leq I^{\max}, \quad \forall j \in \mathcal{C}, i = 1, \dots, b \\ & P_{C,j} \leq P_C^{\max}, \quad P_{D,k} \leq P_D^{\max}, \quad \forall j \in \mathcal{C}, k \in \mathcal{D} \\ & \sum_{k \in \mathcal{D}} x_{k,j} \leq 1, \quad \sum_{j \in \mathcal{C}} x_{k,j} \leq 1, \quad \forall j \in \mathcal{C}, k \in \mathcal{D} \\ & x_{k,j} \in \{0, 1\}, \quad \|\mathbf{w}_j\|^2 = 1, \quad \forall j \in \mathcal{C}, k \in \mathcal{D} \end{aligned}$$

where \mathcal{D} denotes the set of admissible D2D pairs, γ_C^{\min} and γ_D^{\min} are the minimum SINR requirements at the BS and D2D receiver, respectively, ϵ is the maximum probability of the D2D SINR dropping below γ_D^{\min} , and I^{\max} is the worst-case ICI threshold in neighboring cells.⁵ We define that D2D pair k is admissible if it can reuse at least one subchannel from \mathcal{C} .

Note that problem \mathcal{R}_1 is a mixed integer programming problem and is challenging to solve. We develop the solution in two steps, specifically joint power allocation of a CU-D2D pair and CU-D2D matching. Due to orthogonal channelization within each cell, we first focus on the problem of joint power control and beamforming for a CU-D2D pair. Then in Section IV, we describe the CU-D2D matching problem of assigning each admissible D2D pair to reuse a CU's subchannel.

Our goal is to maximize the expected sum rate of the CU and D2D pair by optimizing (P_D, P_C, \mathbf{w}) , under SINR requirements, per-node maximum power, and ICI constraints. The expected sum rate maximization problem is given by

$$\begin{aligned} \mathcal{P}_1 : \quad & \max_{(P_D, P_C, \mathbf{w}: \|\mathbf{w}\|^2=1)} \log_2(1 + \gamma_C) + \mathbb{E}[\log_2(1 + \gamma_D)] \\ \text{subject to} \quad & \gamma_C \geq \gamma_C^{\min}, \quad (4) \\ & \Pr\{\gamma_D \leq \gamma_D^{\min}\} \leq \epsilon, \quad (5) \\ & P_C \leq P_C^{\max}, \quad P_D \leq P_D^{\max}, \quad (6) \\ & \mathbb{E}[P_{I,j}] \leq I^{\max}, \quad j = 1, \dots, b. \quad (7) \end{aligned}$$

⁵We bound ICI in neighboring cells over those subchannels that are used in the desired cell regardless of the number of D2D pairs and CUs in neighboring cells. Our model can be easily extended to set different interference levels to different cells. Let I_j denote the total interference that can be tolerated at destination j . Then we can constrain the interference from each neighboring cell to this cell by setting $I_j^{\max} = \frac{I_j}{N_j}$ where N_j is the number of interfering neighboring cells. Our results hold by replacing I^{\max} with I_j^{\max} .

In the following, we solve optimization problem \mathcal{P}_1 . This problem is non-convex, since both objective function and constraints are non-convex. We solve \mathcal{P}_1 in two steps. First, we need to ensure whether the D2D pair can be admitted to reuse the CU's assigned channel. Then, if the D2D pair is admissible, we attempt to optimize the powers and beam vector to maximize the expected sum rate. We recast the first problem as a feasibility test. Then we obtain the power solution.

III. POWER CONTROL SOLUTION FOR \mathcal{P}_1

A. D2D Admissibility Condition

Following the Nakagami fading model, we assume $|h_D|^2 \sim \Gamma(\alpha_1, \beta_1)$ and $|g_C|^2 \sim \Gamma(\alpha_2, \beta_2)$ where α_1 and α_2 are positive integers and $\{\alpha_1, \beta_1, \alpha_2, \beta_2\}$ are known at the BS. For the ICI channels, we assume $\mathbb{E}[|\mathbf{f}_{D,j}|^2] = \lambda_{D,j}$ and $\mathbb{E}[|\mathbf{f}_{C,j}|^2] = \lambda_{C,j}$ for $j = 1, \dots, b$ where only $\{\lambda_{D,j}\}_{j=1}^b$ and $\{\lambda_{C,j}\}_{j=1}^b$ are known at the BS scheduler.

Given the power constraints, SINR requirements, and ICI constraints, the admissibility of the D2D pair can be determined by solving the feasibility test given by

$$\begin{aligned} & \text{find } \{P_D, P_C, \mathbf{w} : \|\mathbf{w}\|^2 = 1\} \quad (8) \\ & \text{subject to (4), (5), (6), and (7).} \end{aligned}$$

We first obtain the optimal beam vector \mathbf{w} in terms of (P_C, P_D) that maximizes γ_C at the left-hand side of constraint (4). For a given pair of (P_C, P_D) , the optimal beam vector is given by

$$\mathbf{w}^o = \frac{\mathbf{\Lambda}_D^{-1} \mathbf{h}_C}{\|\mathbf{\Lambda}_D^{-1} \mathbf{h}_C\|} \quad (9)$$

where $\mathbf{\Lambda}_D \triangleq \sigma^2 \mathbf{I} + P_D \mathbf{g}_D \mathbf{g}_D^H$.

Substituting (9) into (1), the SINR constraint (4) is given by

$$\frac{P_C \|\mathbf{h}_C\|^2}{\sigma^2} \left(1 - \frac{K_1 P_D \|\mathbf{g}_D\|^2}{P_D \|\mathbf{g}_D\|^2 + \sigma^2}\right) \geq \gamma_C^{\min}. \quad (10)$$

For notation simplicity, for the rest of the section, we denote $x \triangleq P_D$ and $y \triangleq P_C$, and use (x, y) to denote the power pair (P_D, P_C) . Then, the necessary and sufficient condition for the D2D pair to be admissible is given in the following proposition.

Proposition 1: Let $(x_{\bar{i}}, y_{\bar{i}})$ denote the minimum transmission power required to satisfy both minimum SINR requirements. The necessary and sufficient condition for the D2D pair to be admissible is given by

$$0 < x_{\bar{i}} \leq P_D^{\max}, \quad (11)$$

$$0 < y_{\bar{i}} \leq P_C^{\max}, \quad (12)$$

$$\tilde{c}_{1,j} y_{\bar{i}} + \tilde{c}_{2,j} x_{\bar{i}} \leq 1, \quad j = 1, \dots, b \quad (13)$$

where $\tilde{c}_{1,j} \triangleq \lambda_{C,j}/I^{\max}$, $\tilde{c}_{2,j} \triangleq \lambda_{D,j}/I^{\max}$, and $\mathbf{s}_{\bar{i}} \triangleq [x_{\bar{i}} \ y_{\bar{i}}]^T$ is the unique power solution of the following equations

$$y = \alpha \left(1 - \frac{K_1}{1 + K_2/x}\right)^{-1} \quad (14)$$

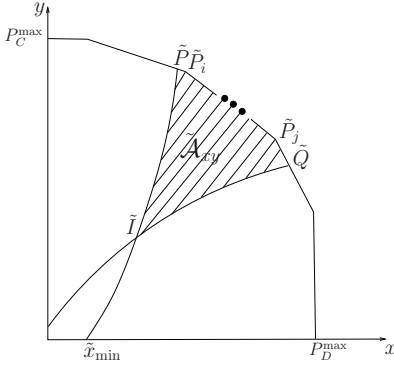


Fig. 2: An example of feasible region for \mathcal{P}_2 .

$$1 - \epsilon = \tilde{K}(\gamma_D^{\min}, x, y) \quad (15)$$

where $\alpha \triangleq \sigma^2 \gamma_C^{\min} / \|\mathbf{h}_C\|^2$, $K_1 \triangleq \frac{\|\mathbf{h}_C^H \mathbf{g}_D\|^2}{\|\mathbf{h}_C\|^2 \|\mathbf{g}_D\|^2}$, $K_2 \triangleq \sigma^2 / \|\mathbf{g}_D\|^2$, and $\tilde{K}(u, x, y) \triangleq \sum_{i=0}^{\alpha_1-1} \frac{\beta_2^{\alpha_2} (\beta_1 u)^i \exp(-\beta_1 u \sigma_D^2 / x)}{y^{\alpha_2} (\alpha_2 - 1)! x^i i!} \sum_{j=0}^i \binom{i}{j} \frac{\sigma_D^{2(i-j)} (\alpha_2 + j - 1)!}{(\beta_2 / y + \beta_1 u / x)^{\alpha_2 + j}}$.

Proof: See Appendix A.

We note that constraints (11) and (12) ensure the maximum powers at the D2D and CU are enough to satisfy both SINR requirements. Constraint (13) ensures the ICI limits can be satisfied. We use an efficient bisection-based method to verify the D2D admissibility, which accelerates solving problem \mathcal{R}_1 .

B. Joint Power Control Solution

Assuming the D2D pair is admissible, we solve \mathcal{P}_1 as an optimal power allocation problem. After substituting \mathbf{w}^o in (9) into (1), and using (x, y) as the power pair, we transform \mathcal{P}_1 into the following equivalent optimization problem:

$$\mathcal{P}_2 : \quad \max_{(x, y)} \bar{\mathcal{R}}(x, y) \quad (16)$$

$$\text{subject to } \tilde{K}(\gamma_D^{\min}, x, y) \geq 1 - \epsilon, \quad (16)$$

$$y \left(1 - \frac{K_1 x}{K_2 + x} \right) l \geq \gamma_C^{\min}, \quad (17)$$

$$y \leq P_C^{\max}, \quad x \leq P_D^{\max}, \quad (18)$$

$$\tilde{c}_{1,j} y + \tilde{c}_{2,j} x \leq 1, \quad j = 1, \dots, b \quad (19)$$

where $\bar{\mathcal{R}}(x, y) = \log_2 \left(\left(1 + y \left(1 - \frac{K_1 x}{K_2 + x} \right) l \right) \right) + \mathbb{E}[\log_2(1 + \gamma_D)]$, $l \triangleq \|\mathbf{h}_C\|^2 / \sigma^2$, and the expected D2D rate has a complicated expression involving numerical integrations (detailed expression is provided in Appendix B).

Note that both the objective function and constraints of problem \mathcal{P}_2 are non-convex. In addition, the objective function involves numerical integrations. Let $\tilde{\mathcal{A}}_{xy}$ denote the feasible solution region of problem \mathcal{P}_2 , i.e., $\tilde{\mathcal{A}}_{xy}$ is non-empty as long as the D2D pair is admissible. An example of $\tilde{\mathcal{A}}_{xy}$ for a specific scenario is shown in Fig. 2. A property of the objective function in \mathcal{P}_2 is provided in the following lemma.

Lemma 1: The optimal power solution pair (x^o, y^o) is at the vertical, horizontal, or a tilted boundary of $\tilde{\mathcal{A}}_{xy}$, given respectively by $x = P_D^{\max}$, $y = P_C^{\max}$, or $\tilde{c}_{1,j} y + \tilde{c}_{2,j} x = 1$ for some j .

Proof: See Appendix C.

Note that Lemma 1 holds for any channel distribution.

The optimal power pair (x^o, y^o) to maximize \mathcal{P}_2 is given in one of two cases: 1) A corner point of the horizontal, vertical, or tilted boundary line segment(s) of $\tilde{\mathcal{A}}_{xy}$; or 2) an interior point of the horizontal, vertical, or tilted boundary line segment(s) of $\tilde{\mathcal{A}}_{xy}$.

In order to solve \mathcal{P}_2 optimally, we need to evaluate the expression of the objective function to find the set of candidate power pairs over each boundary line. Unfortunately, there is no closed-form solution or efficient algorithm to solve those equations. Hence, to avoid such high computational complexity we propose to obtain the powers through approximating the objective function as follows.

We replace $\mathbb{E}[\log_2(1 + \gamma_D)]$ in the objective of \mathcal{P}_2 by the ratio of expectation, i.e., $\log_2 \left(1 + \frac{x \mathbb{E}[\|h_D\|^2]}{\sigma_D^2 + y \mathbb{E}[\|g_C\|^2]} \right)$. In other words, instead of \mathcal{P}_2 , we propose to solve the following problem:

$$\mathcal{P}_3 : \quad \max_{(x, y)} \tilde{\mathcal{R}}(x, y) \quad (19)$$

subject to (16), (17), (18), and (19)

where $\tilde{\mathcal{R}}(x, y) = \log_2 \left(\left(1 + y \left(1 - \frac{K_1 x}{K_2 + x} \right) l \right) \left(1 + \frac{x \alpha_1 / \beta_1}{\sigma_D^2 + y \alpha_2 / \beta_2} \right) \right)$. Note that the objective of \mathcal{P}_3 has a form similar to that of sum rate maximization problem with full CSI. Therefore, \mathcal{P}_3 can be solved by a similar method proposed for the sum rate maximization problem. We term it as the *ROE approximation algorithm*. Although \mathcal{P}_3 and \mathcal{P}_2 are different, we observe through simulation and the upper bound analysis in Section III-D that the ROE algorithm incurs little performance degradation for a wide range of parameter settings.

In [26], under perfect CSI, the solution to the sum rate maximization with the ICI constraint to a single neighboring cell is proposed. We generalize that approach to accommodate multiple ICI constraints to b neighboring cells to solve \mathcal{P}_3 . We first summarize the properties of the optimal solution of \mathcal{P}_3 : The optimal power solution pair is at the vertical, horizontal, or a tilted boundary of $\tilde{\mathcal{A}}_{xy}$ (i.e., $\tilde{c}_{1,j} y + \tilde{c}_{2,j} x = 1$ for some j). If the boundaries of the feasible region $\tilde{\mathcal{A}}_{xy}$ do not include any tilted boundary line segment, then the optimal power pair is at one corner point of the vertical or horizontal boundary. If the boundaries of the feasible region $\tilde{\mathcal{A}}_{xy}$ include $\tilde{c}_{1,j} y + \tilde{c}_{2,j} x = 1$ for some j , then the optimal power pair is given in one of two cases: 1) A corner point of the horizontal, vertical, or tilted boundary line segment(s) of $\tilde{\mathcal{A}}_{xy}$; or 2) an interior point of the tilted boundary line segment(s) of $\tilde{\mathcal{A}}_{xy}$, whose x -coordinate is one of the roots of the following quartic equation

$$e_4 x^4 + e_3 x^3 + e_2 x^2 + e_1 x + e_0 = 0 \quad (20)$$

where the expression of e_i for $i = 0, \dots, 4$ is given in Appendix I. We only need to compute those roots that are feasible. The roots of (20) have *closed-form* expressions.

In sum, our robust solution to solve \mathcal{P}_1 is based on an admissibility test followed by finding candidates for the optimal power solution by an ROE approximation. Those candidates include corner points and interior points of the feasible region, where the interior points are obtained by an efficient root finding algorithm.

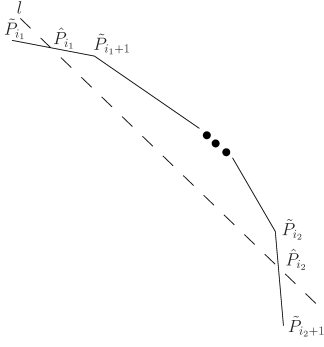


Fig. 3: Intersection of a new tilted line.

C. Algorithm Details

To solve \mathcal{P}_3 , we iteratively compute the feasible solution region by adding each ICI constraint one at a time (a new tilted line on the feasible region). We present a method to efficiently check whether the feasible region is non-empty, thereby testing the admissibility of the D2D pair. Then, the candidates for the optimal power solution are identified and computed through finding the root of equations of the form of (20). We define $\tilde{\mathbf{C}} \triangleq [\tilde{\mathbf{c}}_1 \ \tilde{\mathbf{c}}_2 \ \dots]$ where $\tilde{\mathbf{c}}_i$ is 2×1 vector and columns of $\tilde{\mathbf{C}}$ contain all the corner points of the feasible region based on constraints (18) and (19) and ignoring constraints (16) and (17). We define $\tilde{\mathbf{A}} \triangleq [\tilde{\mathbf{a}}_1 \ \tilde{\mathbf{a}}_2 \ \dots]$ where $\tilde{\mathbf{a}}_i$ is 3×1 vector and columns of $\tilde{\mathbf{A}}$ specify the line segment connecting two consecutive corner points in $\tilde{\mathbf{C}}$. The detailed steps of the algorithm are as follows.

1) *Initialization*: We initialize

$$\tilde{\mathbf{C}} = \begin{bmatrix} 0 & 0 & P_D^{\max} & P_D^{\max} & 0 \\ 0 & P_C^{\max} & P_C^{\max} & 0 & 0 \end{bmatrix}, \quad (21)$$

$$\tilde{\mathbf{A}} = \begin{bmatrix} 1 & 0 & 1 & 0 \\ 0 & 1 & 0 & 1 \\ 0 & P_C^{\max} & P_D^{\max} & 0 \end{bmatrix}. \quad (22)$$

Note that this initial $\tilde{\mathbf{C}}$ is constructed using only constraint (18). The first and last columns of the initial $\tilde{\mathbf{C}}$ are $[0 \ 0]^T$, *i.e.*, the origin coordinates. The other corner points are in the columns of the initial $\tilde{\mathbf{C}}$ in a clock-wise order. The first and last columns of the initial $\tilde{\mathbf{A}}$ ensure that transmission powers are non-negative. For matrix $\tilde{\mathbf{A}}$, the column $\tilde{\mathbf{a}}_i$ is $[\tilde{a}_{i1} \ \tilde{a}_{i2} \ \tilde{a}_{i3}]^T$ when the line segment between $\tilde{\mathbf{c}}_i$ and $\tilde{\mathbf{c}}_{i+1}$ is $\tilde{a}_{i1}x + \tilde{a}_{i2}y = \tilde{a}_{i3}$. The intersection of this line segment and $\tilde{c}_{1,j}y + \tilde{c}_{2,j}x = 1$ is $\tilde{\mathbf{s}}_{i,j} = [\tilde{s}_{x,i,j} \ \tilde{s}_{y,i,j}]^T$ where

$$\tilde{s}_{x,i,j} = \frac{\tilde{a}_{i2} - \tilde{c}_{1,j}\tilde{a}_{i3}}{\tilde{c}_{2,j}\tilde{a}_{i2} - \tilde{c}_{1,j}\tilde{a}_{i1}}, \quad \tilde{s}_{y,i,j} = \frac{\tilde{c}_{2,j}\tilde{a}_{i3} - \tilde{a}_{i1}}{\tilde{c}_{2,j}\tilde{a}_{i2} - \tilde{c}_{1,j}\tilde{a}_{i1}}. \quad (23)$$

We further define

$$\tilde{\mathbf{\Delta}} \triangleq [-\mathbf{I}_2 \ \mathbf{I}_2]^T, \quad \tilde{\mathbf{\delta}} \triangleq [0 \ 0 \ P_D^{\max} \ P_C^{\max}]^T. \quad (24)$$

2) *Admissibility Test*: Let $\tilde{\mathcal{A}}_{xy,j}$ denote the updated feasible region after including ICI constraint j . Then we add a new tilted line l corresponding to ICI constraint $j+1$ as shown in Fig 3. Note that l intersects $\tilde{\mathcal{A}}_{xy,j}$ at exactly two points if there

is any intersection. Assume line l intersects two boundary line segments $\tilde{\mathbf{a}}_{i_1}$ and $\tilde{\mathbf{a}}_{i_2}$ where $\tilde{\mathbf{a}}_{i_1}$ connects the corner points \tilde{P}_{i_1} and \tilde{P}_{i_1+1} , and $\tilde{\mathbf{a}}_{i_2}$ connects the corner points \tilde{P}_{i_2} and \tilde{P}_{i_2+1} with $i_1 < i_2$. Let points \tilde{P}_{i_1} and \tilde{P}_{i_2} be the intersecting points of line l with $\tilde{\mathbf{a}}_{i_1}$ and $\tilde{\mathbf{a}}_{i_2}$, respectively. Since \tilde{P}_{i_1} and \tilde{P}_{i_2} are the corner points of the new feasible region $\tilde{\mathcal{A}}_{xy,j+1}$, we update $\tilde{\mathbf{C}}$ by keeping the corner points $\{\tilde{P}_{i_1}, \tilde{P}_{i_2+1}\}$ and removing $\{\tilde{P}_{i_1+1}, \dots, \tilde{P}_{i_2}\}$, *i.e.*, all the middle points. The new feasible region $\tilde{\mathcal{A}}_{xy,j+1}$ includes $\{\tilde{P}_{i_1}, \tilde{P}_{i_1}, \tilde{P}_{i_2}, \tilde{P}_{i_2+1}\}$. Accordingly, we update the matrices $\tilde{\mathbf{C}}$ and $\tilde{\mathbf{A}}$.

In order to test the admissibility of the D2D pair, we consider the intersection of $\tilde{\mathcal{A}}_{xy,b}$ with the curves associated with minimum SINR requirements (16) and (17). A necessary and sufficient condition for the D2D pair to be admissible is that the solution \mathbf{s}_f in Proposition 1 satisfies $\tilde{\mathbf{\Delta}} \cdot \mathbf{s}_f \leq \tilde{\mathbf{\delta}}$ where $\tilde{\mathbf{\Delta}}$ and $\tilde{\mathbf{\delta}}$ are obtained iteratively through the algorithm. Fig. 2 shows an example of the feasible region. Its boundary may include some tilted, horizontal, or vertical boundary line segments.

3) *Finding Corner Points of Feasible Region*: In order to solve problem \mathcal{P}_3 , we need to find all candidates for the optimal solution. Let \tilde{P} and \tilde{Q} denote the points where the curves $\tilde{I} - \tilde{P}$ and $\tilde{I} - \tilde{Q}$ intersect $\tilde{\mathcal{A}}_{xy,b}$ as shown in Fig. 2. As discussed earlier, the optimal power pair (x^o, y^o) can be one of points $\{\tilde{P}, \tilde{P}_i, \dots, \tilde{P}_j, \tilde{Q}\}$ in this figure. The intersection of curves $\tilde{I} - \tilde{P}$ and $\tilde{I} - \tilde{Q}$ with the horizontal boundary line segment $y = P_C^{\max}$ are given by

$$\tilde{\mathbf{p}}_H = \begin{bmatrix} x_H & P_C^{\max} \end{bmatrix}^T, \quad (25)$$

$$\tilde{\mathbf{q}}_H = \begin{bmatrix} K_2 \left(\frac{K_1}{1 - \alpha/P_C^{\max}} - 1 \right)^{-1} P_C^{\max} \end{bmatrix}^T \quad (26)$$

where x_H is given by solving $1 - \epsilon = \tilde{K}(\gamma_D^{\min}, x_H, P_C^{\max})$ using bisection ($\tilde{K}(\cdot, \cdot, \cdot)$ is defined below (15)). The intersection of curves $\tilde{I} - \tilde{P}$ and $\tilde{I} - \tilde{Q}$ with the vertical boundary line segment $x = P_D^{\max}$ are given by

$$\tilde{\mathbf{p}}_V = \begin{bmatrix} P_D^{\max} & y_V \end{bmatrix}^T, \quad (27)$$

$$\tilde{\mathbf{q}}_V = \begin{bmatrix} P_D^{\max} & \alpha \left(1 - \frac{K_1}{1 + K_2/P_D^{\max}} \right)^{-1} \end{bmatrix}^T \quad (28)$$

where y_V is given by solving $1 - \epsilon = \tilde{K}(\gamma_D^{\min}, P_D^{\max}, y_V)$. The intersections of curves $\tilde{I} - \tilde{P}$ and $\tilde{I} - \tilde{Q}$ with a tilted boundary line segment $\tilde{c}_{1,j}y + \tilde{c}_{2,j}x = 1$ are given by

$$\tilde{\mathbf{p}}_{T,j} = \begin{bmatrix} \tilde{\psi}_{2,j} & \frac{1 - \tilde{c}_{2,j}\tilde{\psi}_{2,j}}{\tilde{c}_{1,j}} \end{bmatrix}^T, \quad (29)$$

$$\tilde{\mathbf{q}}_{T,j} = \begin{bmatrix} \tilde{\psi}_{1,j} & \frac{1 - \tilde{c}_{2,j}\tilde{\psi}_{1,j}}{\tilde{c}_{1,j}} \end{bmatrix}^T \quad (30)$$

where

$$\tilde{\psi}_{1,j} \triangleq \frac{\theta_j + \sqrt{\theta_j^2 - 4\tilde{c}_{2,j}(1 - K_1)K_2(\alpha\tilde{c}_{1,j} - 1)}}{2\tilde{c}_{2,j}(1 - K_1)} \quad (31)$$

with $\theta_j \triangleq 1 - K_1 - \tilde{c}_{2,j}K_2 - \alpha\tilde{c}_{1,j}$, and $\tilde{\psi}_{2,j}$ is given by solving

$$1 - \epsilon = \tilde{K}(\gamma_D^{\min}, \tilde{\psi}_{2,j}, (1 - \tilde{c}_{2,j}\tilde{\psi}_{2,j})/\tilde{c}_{1,j}) \quad (32)$$

using bisection for $j = 1, \dots, b$.

4) *Finding Roots*: Let $\tilde{\mathcal{T}}$ and $\tilde{\mathcal{S}}_j$ denote the sets of all feasible corner points and roots of (20) that meet the range constraint for $\tilde{c}_{1,j}y + \tilde{c}_{2,j}x = 1$, respectively. Then the set of candidate points on the interior of line segment $\tilde{c}_{1,j}y + \tilde{c}_{2,j}x = 1$ is given by

$$\tilde{\mathcal{Z}}_j \triangleq \left\{ [x_r (1 - \tilde{c}_{2,j}x_r)/\tilde{c}_{1,j}]^T : x_r \in \tilde{\mathcal{S}}_j \right\}. \quad (33)$$

Thus, the set of candidate pairs for (x^o, y^o) is given by $\tilde{\mathcal{P}}^o = \tilde{\mathcal{T}} \cup_{j=1}^b \tilde{\mathcal{Z}}_j$.

The steps to solve Problem \mathcal{P}_3 are summarized in Algorithm 1.

Algorithm 1 Maximizing the objective of problem \mathcal{P}_3 (the ROE approximation algorithm)

Input: $\alpha, K_1, K_2, x_H, y_V, \{\tilde{c}_{1,j}\}_{j=1}^b, \{\tilde{c}_{2,j}\}_{j=1}^b, P_C^{\max}, P_D^{\max}$
Output: x^o, y^o , and \mathbf{w}^o

Step 1) Initialization:

1: Set $k = 0$, $\tilde{\mathbf{C}}$ as in (21), $\tilde{\mathbf{A}}$ as in (22), $\tilde{\delta}$ and $\tilde{\Delta}$ as in (24).

Step 2) Admissibility Test:

2: **for** $j = 1 : b$ **do**

3: **for** $i = 1 : n_{\tilde{\mathbf{A}}}$ **do**

4: Compute $\tilde{\mathbf{s}}_{i,j} = [\tilde{s}_{x,i,j} \ \tilde{s}_{y,i,j}]^T$ in (23).

5: **if** $\tilde{\Delta} \cdot \tilde{\mathbf{s}}_{i,j} \preceq \tilde{\delta}$ and $k == 0$ **then**

6: Set $i_1 = i$, $k = 1$, and $\tilde{\mathbf{s}}_1 = \tilde{\mathbf{s}}_{i,j}$.

7: **else if** $\tilde{\Delta} \cdot \tilde{\mathbf{s}}_{i,j} \preceq \tilde{\delta}$ and $k == 1$ **then**

8: Set $i_2 = i$ and $\tilde{\mathbf{s}}_2 = \tilde{\mathbf{s}}_{i,j}$.

9: **end if**

10: **end for**

11: **if** $k > 0$ **then**

12: Set $\tilde{\mathbf{C}}_1 \triangleq \tilde{\mathbf{c}}_{1:i_1}$, $\tilde{\mathbf{C}}_2 \triangleq \tilde{\mathbf{c}}_{i_2+1:n_{\tilde{\mathbf{C}}}}$, $\tilde{\mathbf{A}}_1 \triangleq \tilde{\mathbf{a}}_{1:i_1}$, and $\tilde{\mathbf{A}}_2 \triangleq \tilde{\mathbf{a}}_{i_2+1:n_{\tilde{\mathbf{A}}}}$.

13: Update $\tilde{\mathbf{C}} = [\tilde{\mathbf{C}}_1 \ \tilde{\mathbf{s}}_1 \ \tilde{\mathbf{s}}_2 \ \tilde{\mathbf{C}}_2]$, $\tilde{\mathbf{A}} = [\tilde{\mathbf{A}}_1 \ \tilde{\mathbf{v}} \ \tilde{\mathbf{A}}_2]$ where $\tilde{\mathbf{v}} \triangleq [\tilde{c}_{2,j} \ \tilde{c}_{1,j} \ 1]^T$.

14: Update $\tilde{\Delta} = [\tilde{\Delta}^T \ \tilde{\mathbf{v}}_{1:2}^T]^T$ and $\tilde{\delta} = [\tilde{\delta}^T \ 1]^T$.

15: **end if**

16: **end for**

17: Check $\tilde{\Delta} \cdot \mathbf{s}_{\tilde{\mathbf{I}}} \preceq \tilde{\delta}$ where $\mathbf{s}_{\tilde{\mathbf{I}}}$ is given in Proposition 1.

Step 3) Finding Corner Points:

18: Set $i_s = 2$ and $i_f = n_{\tilde{\mathbf{A}}} - 1$.

19: **if** $\tilde{\mathbf{a}}_{1:2,i_s} == [0 \ 1]^T$ **then**

20: Set $i_s = 3$, $\tilde{\mathbf{p}}_1$ as in (25), and $\tilde{\mathbf{q}}_1$ as in (26).

21: **else if** $\tilde{\mathbf{a}}_{1:2,i_f} == [1 \ 0]^T$ **then**

22: Set $i_f = n_{\tilde{\mathbf{A}}} - 2$, $\tilde{\mathbf{p}}_{n_{\tilde{\mathbf{A}}}-2}$ as in (27), and $\tilde{\mathbf{q}}_{n_{\tilde{\mathbf{A}}}-2}$ as in (28).

23: **end if**

24: **for** $j = i_s : i_f$ **do**

25: Set $\tilde{\mathbf{p}}_{j-1}$ as in (29) and $\tilde{\mathbf{q}}_{j-1}$ as in (30).

26: **end for**

27: Find j_1 and j_2 such that $\tilde{\Delta} \cdot \tilde{\mathbf{p}}_{j_1} \preceq \tilde{\delta}$ and $\tilde{\Delta} \cdot \tilde{\mathbf{q}}_{j_2} \preceq \tilde{\delta}$.

28: Define $\tilde{\mathcal{T}} = \{\tilde{\mathbf{p}}_{j_1}, \tilde{\mathbf{c}}_{j_1+2:j_2+1}, \tilde{\mathbf{q}}_{j_2}\}$ and set $\tilde{\mathcal{P}}^o = \tilde{\mathcal{T}}$.

Step 4) Finding Roots:

29: **for** $k = 1 : n_{\tilde{\mathcal{T}}} - 1$ **do**

30: **if** $\tilde{\mathbf{a}}_{1:2,k+j_1} == [1 \ 0]^T$ or $\tilde{\mathbf{a}}_{1:2,k+j_1} == [0 \ 1]^T$ **then return**

31: **else**

32: Compute $\tilde{\mathcal{Z}}$ in (33) with $\tilde{\mathbf{u}}_{1,k} \leq x_r \leq \tilde{\mathbf{u}}_{1,k+1}$ where

$\tilde{\mathbf{U}} = [\tilde{\mathbf{p}}_{j_1} \ \tilde{\mathbf{c}}_{j_1+2:j_2+1} \ \tilde{\mathbf{q}}_{j_2}]$.

33: Update $\tilde{\mathcal{P}}^o = \tilde{\mathcal{P}}^o \cup \tilde{\mathcal{Z}}$.

34: **end if**

35: **end for**

36: Enumerate among candidate solution set $\tilde{\mathcal{P}}^o$ to find the optimal solution.

37: Obtain the optimal beam vector.

D. An Upper Bound on $\overline{\mathcal{R}}^o$

We have presented our algorithm to solve problem \mathcal{P}_3 exactly. Let (x^*, y^*) denote the optimal solution of \mathcal{P}_3 . Substituting (x^*, y^*) into the objective of \mathcal{P}_2 , we have $\overline{\mathcal{R}}(x^*, y^*) \leq \overline{\mathcal{R}}^o$ where $\overline{\mathcal{R}}^o$ denotes the optimal value of the objective in \mathcal{P}_2 (and \mathcal{P}_1). Since it is difficult to compute $\overline{\mathcal{R}}^o$, we use an upper bound on $\overline{\mathcal{R}}^o$ to evaluate the gap between $\overline{\mathcal{R}}(x^*, y^*)$ and $\overline{\mathcal{R}}^o$.

Proposition 2: Let $\hat{\mathcal{R}}^o$ denote the maximum objective in the following problem. Then, $\overline{\mathcal{R}}^o \leq \hat{\mathcal{R}}^o$.

$$\mathcal{P}_4 : \quad \max_{(x,y)} \hat{\mathcal{R}}(x,y)$$

subject to (16), (17), (18), and (19)

where $\hat{\mathcal{R}}(x,y) = \log_2 \left((1 + y(1 - \frac{K_1 x}{K_2 + x})l) (1 + G \frac{x\alpha_1/\beta_1}{\sigma_D^2 + y\alpha_2/\beta_2}) \right)$, $G = \sup_y (\sigma_D^2 + \alpha_2 y/\beta_2) J(y)$, and $J(y)$ is given in Appendix D.

Proof: See Appendix D.

Note that since the objectives of \mathcal{P}_3 and \mathcal{P}_4 have similar structures, we can simply modify Algorithm 1 to solve \mathcal{P}_4 . Therefore, we can estimate the performance loss due to ROE approximation efficiently.

E. Special Case: Rayleigh Fading Model

As an important special case of Gamma distribution, we consider $|h_D|^2 \sim \exp(\eta_1)$ and $|g_C|^2 \sim \exp(\eta_2)$, which corresponds to the common Rayleigh fading model. Under this model, the solution expression becomes simpler. We provide the solution to \mathcal{P}_1 under Rayleigh fading model, which we refer to as problem \mathcal{Q}_1 .

Following the previous procedure in solving \mathcal{P}_1 , we first determine the admissibility of the D2D pair, and then optimize the powers and beam vector to maximize the expected sum rate.

1) *Admissibility Condition:* Following a similar argument as Section III-A, for a given set of (P_C, P_D) , the optimal beam vector is given by (9). Substituting (9) into (1), the necessary and sufficient condition for the D2D pair to be admissible is given by the following proposition.

Proposition 3: The necessary and sufficient condition for the D2D pair to be admissible is given by (11)–(13) and $\mathbf{s}_{\tilde{\mathbf{I}}} \triangleq [x_{\tilde{\mathbf{I}}} \ y_{\tilde{\mathbf{I}}}]^T$ is the unique power solution of the following equations

$$(14) \text{ and } y = l_1 x \left(\frac{\exp(-l_2/x)}{1 - \epsilon} - 1 \right) \quad (34)$$

where $l_1 = \eta_2/\eta_1/\gamma_D^{\min}$ and $l_2 = \eta_1\sigma_D^2\gamma_D^{\min}$.

Proof: See Appendix E.

2) *Power Control Solution:* Assuming the D2D pair is admissible, after substituting \mathbf{w}^o into (1), we transform \mathcal{P}_1 into the following equivalent problem:

$$\mathcal{Q}_2 : \quad \max_{(x,y)} \overline{\mathcal{R}}(x,y)$$

subject to (E.2), (17), (18), and (19)

where $\overline{\mathcal{R}}(x,y)$ is defined in \mathcal{P}_2 .

Following Lemma 1, the optimal power solution pair (x^o, y^o) is at the vertical, horizontal, or a tilted boundary

of \tilde{A}_{xy} , given respectively by $x = P_D^{\max}$, $y = P_C^{\max}$, or $\tilde{c}_{1,j}y + \tilde{c}_{2,j}x = 1$ for some j . We obtain the close-form of $\mathbb{E}[\log_2(1 + \gamma_D)]$ in Appendix F.

In order to simplify the notations, we change the variables $\hat{x} \triangleq \eta_1 \sigma_D^2 / x$ and $\hat{y} \triangleq \eta_2 \sigma_D^2 / y$ in the following proposition. The vertical boundary line $x = P_D^{\max}$ and horizontal boundary line $y = P_C^{\max}$ can be represented by $\hat{x} = v_1$ and $\hat{y} = v_2$, respectively with $v_1 = \eta_1 \sigma_D^2 / P_D^{\max}$ and $v_2 = \eta_2 \sigma_D^2 / P_C^{\max}$. Similarly, the tilted boundary line $\tilde{c}_{1,j}y + \tilde{c}_{2,j}x = 1$ can be written as $\hat{c}_{1,j}/\hat{y} + \hat{c}_{2,j}/\hat{x} = 1$ with $\hat{c}_{1,j} = \tilde{c}_{1,j}\eta_2\sigma_D^2$ and $\hat{c}_{2,j} = \tilde{c}_{2,j}\eta_1\sigma_D^2$ for $j = 1, \dots, b$.

Proposition 4: The optimal power pair $(\hat{x}^\circ, \hat{y}^\circ)$ to maximize \mathcal{Q}_2 is given in any of the following cases:

- 1) Transformed vertical boundary line: $\hat{x} = v_1$ and \hat{y} is a simple root of the equation

$$\frac{-\hat{\alpha}_3(\hat{y} - v_1)^2}{\hat{y}(\hat{y} + \hat{\alpha}_3)f_V(\hat{y})} + \frac{\hat{y} - v_1(1 + E'(v_1))}{f_V(\hat{y})} - E'(\hat{y}) = 0$$

where $E'(\cdot)$ is defined in Lemma 3, $\hat{\alpha}_3 = l\eta_2\sigma_D^2(1 - K_1P_D^{\max}/(K_2 + P_D^{\max}))$, and $f_V(\hat{y}) = \hat{y}^2 - \hat{y}v_1 - v_1$.

- 2) Transformed horizontal boundary line: $\hat{y} = v_2$ and \hat{x} is a simple root of the equation

$$\frac{-\hat{\beta}\hat{K}_1(v_2 - \hat{x})^2}{f_{1,H}(\hat{x})} + \frac{v_2E'(v_2)}{f_H(\hat{x})} + \frac{v_2(v_2 - \hat{x})}{\hat{x}f_H(\hat{x})} - E'(\hat{x}) = 0$$

where $\hat{\beta} = lP_C^{\max}$, $\hat{K}_1 = K_1\eta_1\sigma_D^2/K_2$, $\hat{K}_2 = \eta_1\sigma_D^2/K_2$, $f_H(\hat{x}) = v_2^2 + v_2 - v_2\hat{x}$, and $f_{1,H}(\hat{x}) = (\hat{K}_2 + \hat{x})((\hat{\beta} + 1)(\hat{K}_2 + \hat{x}) - \hat{K}_1\hat{\beta})f_H(\hat{x})$.

- 3) Transformed tilted boundary line: $\hat{c}_{1,j}/\hat{y} + \hat{c}_{2,j}/\hat{x} = 1$ where \hat{x} is a simple root of the equation

$$f_{1,T}(\hat{x}) + f_{2,T}E'(\hat{x}) - f_{3,T}E'(g_T(\hat{x})) = 0 \quad (35)$$

where $\hat{c}_{1,j} = \eta_2\sigma_D^2\tilde{c}_{1,j}$, $\hat{c}_{2,j} = \eta_1\sigma_D^2\tilde{c}_{2,j}$, $\hat{b}_{1,j} = l/\tilde{c}_{1,j}$, $\hat{b}_{2,j} = l\tilde{c}_{2,j}\eta_1\sigma_D^2/\tilde{c}_{1,j}$, $g_T(\hat{x}) = \frac{\hat{c}_{1,j}\hat{x}}{\hat{x} - \hat{c}_{2,j}}$, $f_{1,T}(\hat{x}) = \frac{\hat{b}_{2,j}\hat{x}^{-2}(1 - \hat{K}_1/(\hat{K}_2 + \hat{x})) + \hat{K}_1/(\hat{K}_2 + \hat{x})^2(\hat{b}_{1,j} - \hat{b}_{2,j}/\hat{x})}{1 + (\hat{b}_{1,j} - \hat{b}_{2,j}/\hat{x})(1 - \hat{K}_1/(\hat{K}_2 + \hat{x}))}$, $\hat{c}_{1,j}/\hat{x}/\hat{w}_j - \hat{c}_{1,j}\hat{c}_{2,j}/(\hat{x} - \hat{c}_{2,j})/\hat{w}_j$, $f_{2,T}(\hat{x}) = \hat{c}_{1,j}/\hat{w}_j^2 + \hat{c}_{1,j}/\hat{w}_j$, $f_{3,T}(\hat{x}) = \hat{c}_{1,j}/\hat{w}_j^2 - \hat{c}_{1,j}\hat{c}_{2,j}/(\hat{x} - \hat{c}_{2,j})^2/\hat{w}_j$, and $\hat{w}_j = \hat{c}_{1,j} + \hat{c}_{2,j} - \hat{x}$.

Proof: See Appendix G.

A numerical equation corresponding to each boundary line should be solved to solve \mathcal{Q}_2 optimally. We are not aware of any efficient algorithm to solve those equations.⁶ To reduce computational complexity, we again use the following approximation to obtain the powers.

Similar to Section III-B, we replace $\mathbb{E}[\log_2(1 + \gamma_D)]$ in the objective of \mathcal{Q}_2 by the ratio of expectation and solve the following problem

$$\mathcal{Q}_3 : \quad \max_{(x,y)} \tilde{\mathcal{R}}(x,y)$$

subject to (E.2), (17), (18), and (19)

where $\tilde{\mathcal{R}}(x,y) = \log_2\left(\left(1 + y\left(1 - \frac{K_1x}{K_2+x}\right)l\right)\left(1 + \frac{x/\eta_1}{\sigma_D^2 + y/\eta_2}\right)\right)$. Note that \mathcal{Q}_3 can be solved by a similar method as ROE

⁶Our extensive simulation results suggest that cases 1 and 2 do not have a valid solution in the specific intervals determined by \tilde{A}_{xy} . However, we still need to solve (35) numerically.

approximation algorithm in Algorithm 1. Through simulation and upper bound analysis in Section III-E4, we verify our approximation leads to a solution close to the optimal one.

3) *Algorithm Details:* The detailed steps of the algorithm to solve \mathcal{Q}_3 different from those in Algorithm 1 are as follows.

- Admissibility test (Line 17 in Algorithm 1): A necessary and sufficient condition for the D2D pair to be admissible is that the solution $\mathbf{s}_{\tilde{I}}$ in Proposition 3 satisfies $\tilde{\Delta} \cdot \mathbf{s}_{\tilde{I}} \preceq \tilde{\delta}$ where $\tilde{\Delta}$ and $\tilde{\delta}$ are obtained iteratively through the algorithm.
- Finding corner points (Lines 20, 22, and 25 in Algorithm 1): The intersection of $\tilde{I} - \tilde{P}$ with the horizontal boundary line segment $y = P_C^{\max}$ is given by (25) where x_H is given by solving $l_1x_H\left(\frac{\exp(-l_2/x_H)}{1-\epsilon} - 1\right) = P_C^{\max}$ using bisection. The intersection of $\tilde{I} - \tilde{P}$ the vertical boundary line segment $x = P_D^{\max}$ is given by

$$\tilde{P}_V = \left[P_D^{\max} l_1 P_D^{\max} \left(\frac{\exp(-l_2/P_D^{\max})}{1-\epsilon} - 1 \right) \right]^T. \quad (36)$$

The intersections of $\tilde{I} - \tilde{P}$ with a tilted boundary line segment $\tilde{c}_{1,j}y + \tilde{c}_{2,j}x = 1$ is given by (29) where $\psi_{2,j}$ is the solution of

$$l_1\tilde{\psi}_{2,j}\left(\frac{\exp(-l_2/\tilde{\psi}_{2,j})}{1-\epsilon} - 1\right) = \frac{1 - \tilde{c}_{2,j}\tilde{\psi}_{2,j}}{\tilde{c}_{1,j}} \quad (37)$$

using bisection for $j = 1, \dots, b$.

4) *An Upper Bound on $\bar{\mathcal{R}}^\circ$:* For benchmarking and evaluating the gap between $\bar{\mathcal{R}}(x^*, y^*)$ and $\bar{\mathcal{R}}^\circ$, we develop an upper bound $\bar{\mathcal{R}}^\circ$.

Proposition 5: An upper bound on the optimal objective of \mathcal{Q}_2 can be obtained by solving the problem

$$\mathcal{Q}_4 : \quad \max_{(x,y)} \hat{\mathcal{R}}(x,y)$$

subject to (E.2), (17), (18), and (19)

where $\hat{\mathcal{R}}(x,y) = \log_2\left(\left(1 + y\left(1 - \frac{K_1x}{K_2+x}\right)l\right)\left(1 + G\frac{x/\eta_1}{\sigma_D^2 + y/\eta_2}\right)\right)$ and $G = \left(1 + \frac{\sigma_D^2\eta_2}{P_C^{\max}}\right)E'\left(\frac{\sigma_D^2\eta_2}{P_C^{\max}}\right) > 1$.

Proof: See Appendix H.

We can solve \mathcal{Q}_4 by tweaking Algorithm 1. Note that $G \rightarrow 1$ as $P_C^{\max} \rightarrow 0$, which can be shown using the following inequalities [33]:

$$0.5 \ln(1 + 2/t) < E'(t) < \ln(1 + 1/t), \quad \text{for all } t > 0. \quad (38)$$

This suggests that the solution of the ROE approximation algorithm is optimal when P_C^{\max} is small enough.

IV. SOLUTION FOR MULTIPLE CUS AND D2D PAIRS

So far, we have provided the power control solution for one CU-D2D pair. We now extend our consideration to the scenario of multiple CUs and D2D pairs to solve \mathcal{R}_1 .

- 1) Determine the admissibility of any D2D pair k to reuse CU j 's subchannel, for $k = 1, \dots, N_D$, $j = 1, \dots, N_C$.
- 2) CU-D2D power solution: For $\forall k, j$, if D2D pair k is admissible to use CU j 's subchannel, we jointly optimize their transmit powers by solving \mathcal{P}_3 using Algorithm 1.

3) CU-D2D matching: We solve the CU-D2D matching problem to optimally assign each admissible D2D pair to a CU and maximize the objective of \mathcal{R}_1 . In particular, we define a bipartite graph between CUs and D2D pairs. Each edge between a D2D pair and a CU indicates that the pairing of the D2D pair and the CU is feasible. The weight of the edge is given by the expected sum rate of the D2D pair and the CU, which is obtained in Step 2. This CU-D2D matching problem, to maximize the expected sum rate, can be solved by the well-known Hungarian algorithm in polynomial time [34].

The optimal CU-D2D matching in Step 3 above requires computing a power control solution for each admissible CU-D2D pair. We can further reduce the computational complexity of this step by using the following suboptimal CU-D2D matching schemes. Instead of the expected sum rate, we define the cost on an edge between D2D pair k and CU j in the bipartite graph as one of the two choices below:

- *Suboptimal CU-D2D matching A*: the intra-cell interference channel gain between CU j and D2D receiver k , i.e., $|g_{j,k}|$;
- *Suboptimal CU-D2D matching B*: the weight of CU transmit power in the ICI constraint.⁷

We will show through simulation that these two approximate matching schemes often perform close to the jointly optimal matching for \mathcal{R}_1 .

Finally, based on the upper bound in \mathcal{P}_4 , an upper bound on the optimal objective of \mathcal{R}_1 is given by

$$\mathcal{R}_1^o \leq \sum_{j \in \mathcal{C}} \hat{\mathcal{R}}(P_{D,k_j}^*, P_{C,j}^*) \quad (39)$$

where $(P_{D,k_j}^*, P_{C,j}^*)$ is the optimal solution of \mathcal{P}_4 for CU j and D2D k_j with $x_{k_j,j}^* = 1$.

In this paper, our goal is to maximize the total weight in a weighted bipartite graph. While we focus on settings where the users do not deviate from the matching scheme, in settings with selfish users, we can use alternative algorithms that guarantee *near optimal* and *stable* matching solutions [35], which is an interesting problem for future work.

V. NUMERICAL RESULTS

We provide numerical results to illustrate the performance of Algorithm 1, with respect to (w.r.t.) the original problems \mathcal{P}_1 and \mathcal{Q}_1 , respectively, along with the CU-D2D matching methods presented in Section IV. The number of neighboring cells is $b = 6$. The cell radius is $d_0 = 0.5$ km and the D2D distance is denoted by d_D . We set $\sigma^2 = \sigma_D^2 = -103$ dBm, $\gamma_C^{\min} = \gamma_D^{\min} = 3$ dB, $P_C^{\max} = P_D^{\max} = P^{\max}$, $\epsilon = 0.1$, and $I_0^{\max} = NI_0$ where I_0 is the ICI threshold reference and $I_0/\sigma^2 = 5$ dB.⁸ We use 5000 channel realizations to evaluate the average performance.

⁷When all ICI constraints are replaced with a single ICI constraint.

⁸In practice, cell-edge users can experience less than 0 dB SINR, but D2D communication should not share spectrum with (and hence create extra interference to) CUs with very low SINR. We have selected a lower bound of 3 dB such that CUs and D2D pairs near the cell edge experience reasonable quality of service. Our system modelling in this section follows the parameters specified in [2].

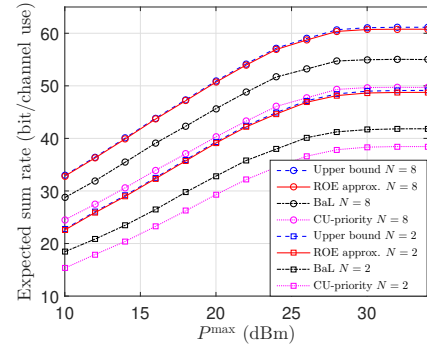


Fig. 4: The expected sum rate with $d_D/d_0 = 0.1$.

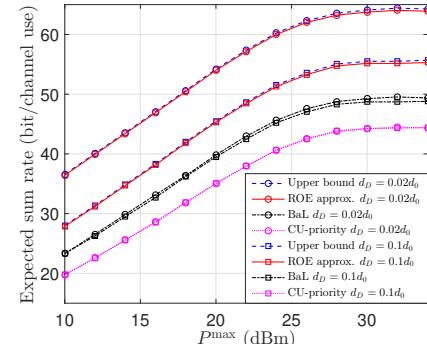


Fig. 5: The expected sum rate with $N = 4$.

For performance comparison, we use the upper bound developed in Section III-E4. Furthermore, we consider two baseline algorithms: 1) *Boost-and-limit (BaL) heuristic*, where the power solution $[x_{\bar{i}} \ y_{\bar{j}}]^T$ is boosted proportionally with a common factor ζ_{\max} such that either the maximum power constraint (18) or the ICI limit (i.e., (19) under partial CSI) is met with equality, i.e., further boosting the powers would violate at least one constraint. Note that the scheduling BS can easily compute this unique power solution and then boost the power of the CU and D2D pair until either the maximum power is achieved or a neighboring cell alerts regarding the ICI level. 2) *CU-priority heuristic*, where a corner point of the feasible region is selected to maximize the SINR of the CU. It selects the maximum feasible CU power with the minimum feasible D2D power.

A. Partial CSI with Nakagami Fading

In this section, we assume $|h_D|^2 \sim \Gamma(5, \beta_1)$ and $|g_C|^2 \sim \Gamma(5, \beta_2)$ with path loss $128.1 + 37.6 \log_{10}(d)$ and $\beta = 5/(\text{channel gain})$. We consider 5 CUs and one D2D pair that are randomly dropped in a cell of interest. The BS coordinates D2D communication by associating the D2D pair with a CU to achieve the maximum expected sum rate.

We first evaluate how the expected sum rate changes with the maximum power P^{\max} , under Algorithm 1 and both baseline algorithms in Fig. 4 for $N = 2$ and 8. We observe two regimes. When the expected sum rate is an increasing function of P^{\max} (Regime 1), the ICI is relatively weak, and the feasible region is not affected by the ICI constraint. As

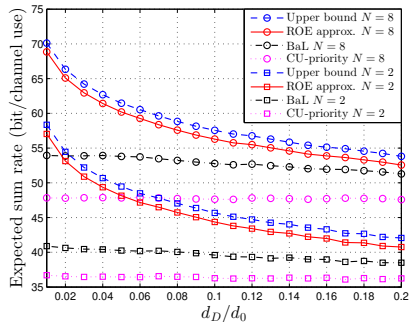


Fig. 6: The expected sum rate with $P^{\max} = 24$ dBm.

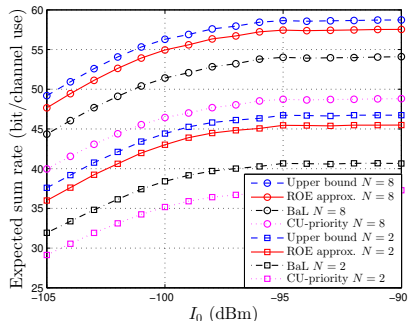


Fig. 7: The expected sum rate with $d_D/d_0 = 0.1$ and $P^{\max} = 24$ dBm.

as a result, the expected sum rate increases linearly with P^{\max} . When the expected sum rate converges (Regime 2), the ICI is relatively strong, and the feasible region is not changed by P^{\max} . Hence, the expected sum rate is controlled by the fixed ICI threshold. It can be seen that the proposed ROE algorithm significantly outperforms the BaL and CU-priority heuristic algorithms for all values of N . Furthermore, the gap between the ROE algorithm and the upper bound is small, at less than 1% of the optimal expected sum rate.

To study the effect of the D2D distance on the performance, the expected sum rate versus P^{\max} for $d_D/d_0 = 0.02$ and 0.1 is shown in Fig. 5. We set $N = 4$. For the ROE algorithm, the expected sum rate improves significantly as d_D/d_0 decreases. However, the performance of the CU-priority heuristic is not sensitive to d_D/d_0 . This is because the proposed ROE algorithm results in a significant rate improvement when the D2D channel is very strong, *i.e.*, the D2D distance is small.

B. Partial CSI with Rayleigh Fading

In this section, we assume Rayleigh fading for each channel with the same path loss as Section V-A. The expected sum rate versus the normalized D2D distance d_D/d_0 for $N = 2$ and 8 is shown in Fig. 6. We observe that, when the D2D channel is strong, *i.e.*, the D2D distance is small, significant expected sum rate is achievable even while knowing only partial CSI. We investigate the effect of the ICI threshold reference I_0 on performance. The expected sum rate versus I_0 is demonstrated in Figs. 7 for $d_D/d_0 = 0.1$, $P^{\max} = 24$ dBm, and $N = 2$ and 8 . We observe that the expected sum rate improves when I_0 increases. For small I_0 values, the expected sum rate

P^{\max}	20	22	24	26	28	30
Opt.	45.6879	49.1297	51.9008	54.1057	55.2725	55.8749
ROE	45.6879	49.1297	51.9001	54.1031	55.2639	55.8623

TABLE I: Expected sum rate (bit/channel use) versus P^{\max} (dBm).

P^{\max}	10	15	20
Upper bound	101.8	117.2	132.4
ROE pow. + opt. match.	100.7	116.0	130.9
BaL. pow. + opt. match.	59.7	69.4	83.7
CU-priority. pow. + opt. match.	45.5	51.4	61.6
ROE pow. + subopt. match. A	94.8	110.6	126.5
ROE pow. + subopt. match. B	89.2	104.9	117.1

TABLE II: Expected sum rate (bit/channel use) versus P^{\max} (dBm) with 7 CU-D2D pairs.

is an increasing function of I_0 since the ICI is relatively strong (Regime 2). As I_0 increases, the ICI constraint becomes inactive (Regime 1) and the expected sum rate converges due to the fixed P^{\max} .

In order to more precisely quantify the performance loss due to the ROE approximation, the expected sum rate versus P^{\max} under ROE algorithm and the optimal power control algorithm obtained by an exhaustive search, for $d_D/d_0 = 0.1$ and $N = 4$, is shown in Table I. We observe that the performance of the ROE algorithm is close to that of optimal power control. In particular, in Regime 1 the performance of both power control schemes overlap. Hence, the ROE approximation algorithm offers nearly optimal performance with drastically reduced computational complexity.

C. Multiple CUs and D2D Pairs with Nakagami Fading

We now consider multiple CUs and D2D pairs in the cell of interest as discussed in Section IV, assuming partial CSI with Nakagami fading as described in Section V-A. We obtain ROE approximation power control solution for the expected sum rate maximization of CU-D2D pairs by Algorithm 1. Seven CUs and three D2D pairs are randomly dropped in the cell. We set $N = 4$ and $d_D/d_0 = 0.1$. We consider proposed CU-D2D matching schemes in Section IV and compare performance of the following schemes: 1) The proposed ROE power control and optimal CU-D2D matching; 2) Upper bound on the optimal objective of \mathcal{R}_1 in (39); 3) BaL heuristic power control and optimal CU-D2D matching; 4) CU-priority heuristic power control and optimal CU-D2D matching; 5) ROE power control and suboptimal CU-D2D matching A; 6) ROE power control and suboptimal CU-D2D matching B.

In Table II, we show the expected sum rate versus P^{\max} by the ROE power control scheme and the baselines. We observe that the ROE power control with optimal CU selection outperforms the BaL and CU-priority heuristics significantly. The performance of the ROE power control and *suboptimal CU-D2D matching A* is close to the optimal CU-D2D matching, which shows that there is a room for reducing the computational complexity of CU-D2D matching in large-scale settings. This happens because using CU-D2D matching A leads to substantial D2D gain by limiting the intra-cell interference caused by a CU to the matched D2D receiver.

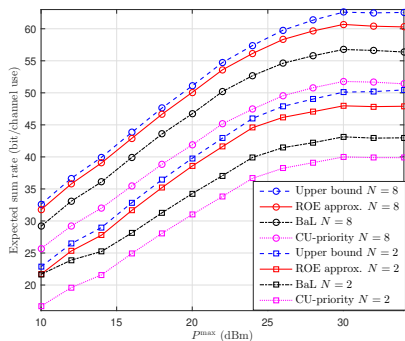


Fig. 8: The expected sum rate under ($d_D/d_0 = 0.1, b = 6$).

Finally, under optimal CU-D2D matching, there is a negligible gap between the proposed ROE power control and the upper bound.

D. Extension to Scenarios with Mobile D2D

We now consider scenarios with mobile D2D pairs similar to the model considered in [12]. Please note that we assume perfect CSI only for channels from the D2D transmitter to the BS. Assuming the D2D pairs are moving with similar velocity, and thus relatively static to each other, we use the first-order Gauss-Markov process to model the interference channel from each D2D to BS, and assume only the estimate of this channel is available. Note that we can modify our proposed solution to solve problem \mathcal{R}_1 , which is based on Algorithm 1 using estimated channels such that the modified algorithm can solve the new problem. Intuitively, after solving the power control problem, if the CU SINR constraint is not met (based on the actual channel including the error term caused by the Doppler effect), D2D power is scaled down to meet that constraint. This modification may cause a slight violation of the probabilistic D2D SINR constraint. However, it ensures that CU SINR and ICI constraints are met. In practice, one might use sufficiently small $\epsilon' < \epsilon$ for some error margin due to estimation error.

We evaluate how the expected sum rate changes with the maximum power P^{\max} , under our proposed algorithm and both baseline algorithms in Fig. 8 for $N = 2$ and 8. We simulate a scenario with a mobile D2D using the parameters in [12]. In particular, the carrier frequency, vehicle speed, and channel feedback latency are set to 2 GHz, 60 km/h, and 0.5 ms, respectively. We compare our proposed algorithm with BaL and CU-priority baselines along with an upper bound, which assumes perfect knowledge of interference channels from D2D to BS and solves a problem with an upper bound on the original objective as explained in Proposition 5. We observe that the proposed algorithm significantly outperforms the baselines for all values of N . Furthermore, the gap between the proposed algorithm and the upper bound is small. Finally, we observed that the probability of D2D SINR violation is less than 1% in all our experiments related to D2D with mobility.

E. Computational Complexity

In Table III, we compare the computational complexity of different algorithms. Please note that we compare complexity

of power control (with one CU and one D2D pair) and CU-D2D matching schemes separately. In Table III, ϵ and $q(b, \epsilon)$ denote the bisection tolerance and the complexity of the power control algorithm. In this analysis, we assume $N_C = N_D = N_U$. We observe that our proposed algorithm with optimal CU-D2D matching have polynomial complexity w.r.t. b and N_U .

VI. CONCLUSION

We have studied the problem of CUs and D2D pairs sharing the uplink cellular spectrum for expected sum rate maximization. In a fading environment, we consider probabilistic constraints representing minimum SINR requirements, per-node maximum power, and ICI constraints in multiple neighboring cells. Our model considers receive beamforming at the BS, and a partial CSI scenario when some CSI is available only in terms of statistics. This is a valid model for D2D-based V2X communication in IoT where full CSI is not available due to substantial signaling overhead. We obtain a simple feasibility test to determine whether a D2D pair can reuse the channel resource of a CU. An efficient robust power control algorithm based on ROE approximation has been developed to obtain the transmit powers of the CU and D2D transmitter, along with an upper bound on the maximum expected sum rate. We have further integrated the proposed power control solution with different CU-D2D matching schemes to obtain the overall solution for multiple CU-D2D pairs. Numerical results demonstrate that the proposed algorithm is close to the upper bound.

MIMO is expected to be one of the main technologies of 5G systems and beyond. However, CSI acquisition at the BS is the main challenge in MIMO scenarios. It is interesting to study the problem of jointly optimizing MIMO and D2D power control as a future work.

APPENDIX A: PROOF OF PROPOSITION 1

Proof: We first obtain the cumulative distribution function for random variable $Z = \frac{X}{\sigma_D^2 + Y}$ where $X \sim \Gamma(\alpha_1, \beta_1/x)$ and $Y \sim \Gamma(\alpha_2, \beta_2/y)$.

$$\begin{aligned} F_Z(z) &= \Pr \left\{ \frac{X}{\sigma_D^2 + Y} \leq z \right\} = \int_0^\infty f_Y(t) F_X(z(\sigma_D^2 + t)) dt \\ &= \int_0^\infty \frac{\beta_2^{\alpha_2} t^{\alpha_2-1} \exp(-\beta_2 t/y)}{y^{\alpha_2} (\alpha_2 - 1)!} (1 - h_1(t)) dt \\ &= 1 - \tilde{K}(z, x, y) \end{aligned}$$

where $h_1(t) = \sum_{i=0}^{\alpha_1-1} \frac{(\beta_1 z(\sigma_D^2 + t))^i}{x^i i!} \exp(-\beta_1 z(\sigma_D^2 + t)/x)$ and $\tilde{K}(\cdot, \cdot, \cdot)$ is defined in (15). The constraint (5) can be written as $F_Z(\gamma_D^{\min}) \leq \epsilon$, i.e.,

$$\tilde{K}(\gamma_D^{\min}, x, y) \geq 1 - \epsilon. \quad (\text{A.1})$$

The D2D SINR requirement (A.1) can be satisfied only if

$$x \geq \tilde{x}_{\min} \quad (\text{A.2})$$

where \tilde{x}_{\min} is the unique solution of $F_X(\gamma_D^{\min} \sigma_D^2) = \epsilon$, i.e.,

$$\sum_{i=0}^{\alpha_1-1} \frac{(\beta_1 \gamma_D^{\min} \sigma_D^2)^i \exp(-\beta_1 \gamma_D^{\min} \sigma_D^2/x)}{x^i i!} = 1 - \epsilon, \quad (\text{A.3})$$

Power control (Partial CSI)			CU-D2D matching		
ROE	BaL	CU-priority	Opt.	Subopt. A	Subopt. B
$O(b^2 + b \log(1/\varepsilon))$	$O(b + \log(1/\varepsilon))$	$O(b^2 + b \log(1/\varepsilon))$	$O(N_U^3 + N_U^2 q(b, \varepsilon))$	$O(N_U^3)$	$O(N_U^3)$

TABLE III: The comparison of computational complexity.

which can be obtained efficiently using a bisection search algorithm. Not that $F_X(\gamma_D^{\min} \sigma_D^2)$ is monotonically decreasing w.r.t. x . ■

APPENDIX B: EXPECTED D2D RATE

Lemma 2: The expected D2D rate is given by (B.1) where $I_{i,j}(x, y) = \int_{\beta_1 \sigma_D^2/x}^{\infty} t^{i+j} E_1(t) \exp(-(\beta_2 x/(\beta_1 y) - 1)t) dt$ and $E_1(x) = \int_x^{\infty} \exp(-t)/t dt$.

Proof: Since $|h_D|^2 \sim \Gamma(\alpha_1, \beta_1)$ and $|g_C|^2 \sim \Gamma(\alpha_2, \beta_2)$, we can obtain $\mathbb{E}[\log_2(1 + \gamma_D)]$ by taking a double integral as follows:

$$\mathbb{E}[\ln(1 + \gamma_D)] = \int_0^{\infty} \int_0^{\infty} \ln\left(1 + \frac{xu}{\sigma_D^2 + yv}\right) g(u, v) du dv$$

where $g(u, v) = \frac{\beta_1^{\alpha_1} u^{\alpha_1-1} \exp(-\beta_1 u)}{(\alpha_1 - 1)! \beta_2^{\alpha_2} v^{\alpha_2-1} \exp(-\beta_2 v) (\alpha_2 - 1)!}$. We then use the following equality [36]:

$$\int_0^{\infty} \frac{t^n \exp(-\mu t)}{t + \beta} dt = (-\beta)^n E'(\beta \mu) + \sum_{k=1}^n (k-1)! (-\beta)^{n-k} \mu^{-k} \quad (\text{B.2})$$

where $E'(x) = \exp(x) E_1(x)$. Using (B.2), $\mathbb{E}[\ln(1 + \gamma_D)]$ can be obtained using a single integral as

$$\mathbb{E}[\ln(1 + \gamma_D)] = \int_0^{\infty} \beta_2^{\alpha_2} v^{\alpha_2-1} W(v) \exp(-\beta_2 v) / (\alpha_2 - 1)! dv$$

where $W(v) = \sum_{i=0}^{\alpha_1-1} \beta_1^i / i! ((-1)^i (\tilde{v})^i E'(\tilde{v} \beta_1) + \sum_{k=1}^i (k-1)! (-\tilde{v})^{i-k} \beta_1^{-k})$ and $\tilde{v} = (\sigma_D^2 + yv)/x$. ■

APPENDIX C: PROOF OF LEMMA 1

Proof: Given any (x, y) in the interior of $\tilde{\mathcal{A}}_{xy}$, there exists $\zeta > 1$, such that $(\zeta x, \zeta y) \in \tilde{\mathcal{A}}_{xy}$. We show that $\overline{\mathcal{R}}(\zeta x, \zeta y) > \overline{\mathcal{R}}(x, y)$ for any $\zeta > 1$. Note that the objective function in \mathcal{P}_2 can be written as $\overline{\mathcal{R}}(x, y) = \mathbb{E}[\log_2(\Omega_{x,y})]$ where

$$\Omega_{x,y} \triangleq \left(1 + y \left(1 - \frac{K_1 x}{K_2 + x}\right) l\right) \left(1 + \frac{x |h_D|^2}{\sigma_D^2 + y |g_C|^2}\right). \quad (\text{C.1})$$

For any realization of random channels $\{h_D, g_C\}$, we have $\Omega_{\zeta x, \zeta y} > \Omega_{x,y}$ following the similar arguments in [26, Lemma 2]. Then we have $\overline{\mathcal{R}}(\zeta x, \zeta y) > \overline{\mathcal{R}}(x, y)$ since $\log_2(\cdot)$ is a monotonically increasing function. As a result, the optimal power pair (x^o, y^o) cannot be in the interior of $\tilde{\mathcal{A}}_{xy}$. ■

APPENDIX D: PROOF OF PROPOSITION 2

Proof: We consider two random variables $Z_1 \triangleq x \mathbb{E}[|h_D|^2]$ and $Z_2 \triangleq \sigma_D^2 + y \mathbb{E}[|g_C|^2]$ for notation simplicity. First, we show the following inequality holds:

$$\frac{\mathbb{E}[Z_1]}{\mathbb{E}[Z_2]} \leq \mathbb{E}\left[\frac{Z_1}{Z_2}\right] = \frac{\mathbb{E}[Z_1]}{\mathbb{E}[Z_2]} \left(\sigma_D^2 + \frac{\alpha_2 y}{\beta_2}\right) J(y) \quad (\text{D.1})$$

where $J(y) = \frac{\beta_2^{\alpha_2} \exp(\sigma_D^2 \beta_2 / y)}{(\alpha_2 - 1)! y^{\alpha_2}} \left((-\sigma_D^2)^{\alpha_2-1} E_1(\sigma_D^2 \beta_2 / y) + \sum_{i=1}^{\alpha_2-1} (-\sigma_D^2)^{\alpha_2-1-i} (y/\beta_2)^i (\alpha_2 - 1)! \bar{\Gamma}(i, \sigma_D^2 \beta_2 / y) \right)$ and $\bar{\Gamma}(s, x) = \int_x^{\infty} t^{s-1} \exp(-t) dt$ is the upper incomplete gamma function.

Note that Z_1 and Z_2 are independent random variables. Hence, we have

$$\mathbb{E}\left[\frac{Z_1}{Z_2}\right] = \mathbb{E}[Z_1] \mathbb{E}\left[\frac{1}{Z_2}\right] \geq \frac{\mathbb{E}[Z_1]}{\mathbb{E}[Z_2]} \quad (\text{D.2})$$

by Jensen's inequality.

We can obtain $\mathbb{E}[1/Z_2]$ as follows:

$$\begin{aligned} \mathbb{E}\left[\frac{1}{Z_2}\right] &= \int_0^{\infty} \frac{\beta_2^{\alpha_2}}{(\sigma_D^2 + v) y^{\alpha_2} (\alpha_2 - 1)!} v^{\alpha_2-1} \exp(-\beta_2 v / y) dv \\ &= \frac{\beta_2^{\alpha_2} \exp(\beta_2 \sigma_D^2 / y)}{(\alpha_2 - 1)! y^{\alpha_2}} \int_{\sigma_D^2}^{\infty} \sum_{i=0}^{\alpha_2-1} \binom{\alpha_2-1}{i} t^{i-1} \\ &\quad \cdot (-\sigma_D^2)^{\alpha_2-1-i} \exp(-\beta_2 t / y) dt \\ &= J(y). \end{aligned} \quad (\text{D.3})$$

Note that for all (x, y) , we have

$$\mathbb{E}\left[\frac{Z_1}{Z_2}\right] < \frac{\mathbb{E}[Z_1]}{\mathbb{E}[Z_2]} \sup(\sigma_D^2 + \frac{\alpha_2 y}{\beta_2}) J(y). \quad (\text{D.4})$$

Finally, $\mathbb{E}[\log_2(1 + Z_1/Z_2)] \leq \log_2(1 + \mathbb{E}[Z_1/Z_2])$ for any given (x, y) due to Jensen's inequality. Hence, the optimal objective of \mathcal{P}_4 is an upper bound on the objective of \mathcal{P}_2 . ■

APPENDIX E: PROOF OF PROPOSITION 3

Proof: We first obtain the cumulative distribution function for random variable $Z = \frac{X}{\sigma_D^2 + Y}$ where $X \sim \exp(\eta_1/x)$ and $Y \sim \exp(\eta_2/y)$.

$$\begin{aligned} F_Z(z) &= \Pr\left\{\frac{X}{\sigma_D^2 + Y} \leq z\right\} = \int_0^{\infty} f_Y(t) F_X(z(\sigma_D^2 + t)) dt \\ &= \int_0^{\infty} \frac{\eta_2 \exp(-\eta_2 t / y)}{y} (1 - \exp(-\eta_1 z(\sigma_D^2 + t)/x)) dt \\ &= 1 - \frac{\eta_2 \exp(-\eta_1 z \sigma_D^2 / x)}{\eta_1 z y / x + \eta_2}. \end{aligned} \quad (\text{E.1})$$

The constraint (5) can be written as $F_Z(\gamma_D^{\min}) \leq \epsilon$, i.e.,

$$y \leq l_1 x \left(\frac{\exp(-l_2/x)}{1 - \epsilon} - 1 \right). \quad (\text{E.2})$$

It is not difficult to show that $g(x) = l_1 x \left(\frac{\exp(-l_2/x)}{1 - \epsilon} - 1 \right)$ is a convex and increasing function of x . Furthermore, the D2D SINR requirement (E.2) can be satisfied only if

$$x \geq \tilde{x}_{\min} \triangleq \frac{-\eta_1 \sigma_D^2 \gamma_D^{\min}}{\ln(1 - \epsilon)}. \quad (\text{E.3})$$

$$\begin{aligned} \mathbb{E}[\log_2(1 + \gamma_D)] &= \log_2(e) \sum_{i=0}^{\alpha_1-1} \frac{\beta_2^{\alpha_2}}{(\alpha_2-1)!i!} \left((-1)^i \exp(\beta_2 \sigma_D^2/y) \sum_{j=0}^{\alpha_2-1} \binom{\alpha_2-1}{j} (x/(\beta_1 y))^{j+1} I_{i,j}(x, y) (-\sigma_D^2/y)^{\alpha_2-1-j} \right. \\ &\quad \left. + \sum_{k=1}^i (k-1)! (-\beta_1/x)^{i-k} \sum_{j=0}^{i-k} \binom{i-k}{j} y^j \sigma_D^{2(i-k-j)} \frac{(\alpha_2+j-1)!}{\beta_2^{\alpha_2+j}} \right) \end{aligned} \quad (\text{B.1})$$

Considering both (10) and (E.2) with equality, the power solution is given by $(x_{\tilde{j}}, y_{\tilde{j}})$. Note that $x_{\tilde{j}}$ is the solution of

$$\alpha \left(1 - \frac{K_1}{1 + K_2/x} \right)^{-1} = l_1 x \left(\frac{\exp(-l_2/x)}{1 - \epsilon} - 1 \right), \quad (\text{E.4})$$

which can be obtained efficiently using a bisection search algorithm within the range $\tilde{x}_{\min} \leq x \leq P_D^{\max}$. We denote the right-hand side of (14) and (34) by $f_1(x)$ and $f_2(x)$, respectively. Note that $f_1(\tilde{x}_{\min}) > f_2(\tilde{x}_{\min})$ and $f_1(x)$ is concave, while $f_2(x)$ is convex. Hence, the power solution from the system of equations (14) and (34) is unique. ■

APPENDIX F: PROOF OF LEMMA 3

Lemma 3: The expected D2D rate is given by

$$\mathbb{E}[\log_2(1 + \gamma_D)] = \frac{\eta_2 x \log_2(e)}{\eta_1 y - \eta_2 x} (E'(\eta_2 \sigma_D^2/y) - E'(\eta_1 \sigma_D^2/x))$$

where $E'(x) = \exp(x) \int_x^\infty \exp(-t)/t dt$.

Proof: Since $|h_D|^2 \sim \exp(\eta_1)$ and $|g_C|^2 \sim \exp(\eta_2)$, we can obtain $\mathbb{E}[\log_2(1 + \gamma_D)]$ by taking a double integral as follows:

$$\begin{aligned} \mathbb{E}[\ln(1 + \gamma_D)] &= \int_0^\infty \int_0^\infty \ln \left(1 + \frac{xu}{\sigma_D^2 + yv} \right) f(u, v) du dv \\ &= \int_0^\infty \int_0^\infty \frac{\eta_2 x \exp(-\eta_1 u - \eta_2 v)}{\sigma_D^2 + yv + xu} du dv \\ &= \int_0^\infty E'(\eta_1(\sigma_D^2 + yv)/x) \eta_2 \exp(-\eta_2 v) dv \\ &= \frac{\eta_2 x}{\eta_1 y} \int_{\frac{\eta_1 \sigma_D^2}{x}}^\infty E'(t) \exp \left(-\frac{\eta_2 x}{\eta_1 y} t + \frac{\eta_2 \sigma_D^2}{y} \right) dt \\ &= \frac{\eta_2 x}{\eta_1 y - \eta_2 x} \left(E' \left(\frac{\eta_2 \sigma_D^2}{y} \right) - E' \left(\frac{\eta_1 \sigma_D^2}{x} \right) \right) \end{aligned}$$

where $f(u, v) \triangleq \eta_1 \exp(-\eta_1 u) \eta_2 \exp(-\eta_2 v)$. ■

APPENDIX G: PROOF OF PROPOSITION 4

Proof: By Lemma 1, the optimal power solution pair $(\hat{x}^\circ, \hat{y}^\circ)$ to maximize \mathcal{P}_2 is given by a corner point or an interior point of the horizontal, vertical, or tilted boundary line segment(s) of $\tilde{\mathcal{A}}_{xy}$. If $(\hat{x}^\circ, \hat{y}^\circ)$ is an interior point, we prove only for the case of tilted boundary line. The other cases can be proved similarly. If ICI constraint j in (19) is active at optimality, the optimal power is the solution of the following optimization problem

$$\max_{(\hat{x}, \hat{y})} \ln \left(1 + \frac{\hat{b}}{\hat{y}} \left(1 - \frac{\hat{K}_1}{\hat{K}_2 + \hat{x}} \right) \right) + \frac{\hat{y}(E'(\hat{x}) - E'(\hat{y}))}{\hat{y} - \hat{x}}$$

subject to $\hat{c}_{1,j}/\hat{y} + \hat{c}_{2,j}/\hat{x} = 1$

where $\hat{b} \triangleq l \eta_2 \sigma_D^2$ and $E'(\cdot)$ is defined in Lemma 3. Substituting $\hat{y} = \frac{\hat{c}_{1,j} \hat{x}}{\hat{x} - \hat{c}_{2,j}}$ into the objective function above, we have $\max_x \hat{\mathcal{R}}(\hat{x})$, where $\hat{\mathcal{R}}(\hat{x}) \triangleq \ln \left(1 + \frac{\hat{b}}{\hat{c}_{1,j} - \hat{c}_{2,j}/\hat{x}} \left(1 - \frac{\hat{K}_1}{\hat{K}_2 + \hat{x}} \right) \right) + \frac{\hat{c}_{1,j} (\exp(\hat{x}) E_1(\hat{x}) - \exp(g_T(\hat{x})) E_1(g_T(\hat{x})))}{\hat{c}_{1,j} + \hat{c}_{2,j} - \hat{x}}$. Since $\hat{\mathcal{R}}(\hat{x})$ is continuous and has a first-order derivative, the optimum \hat{x}° is either an end point of the interval defined by $\tilde{\mathcal{A}}_{xy}$ or obtained by solving $d\hat{\mathcal{R}}(\hat{x})/d\hat{x} = 0$, which results in the equation in (35). ■

APPENDIX H: PROOF OF PROPOSITION 5

Proof: From the proof of Proposition 2 and using the same Z_1 and Z_2 defined there, the following inequality holds:

$$\frac{\mathbb{E}[Z_1]}{\mathbb{E}[Z_2]} \leq \mathbb{E} \left[\frac{Z_1}{Z_2} \right] = \frac{\mathbb{E}[Z_1]}{\mathbb{E}[Z_2]} \left(1 + \frac{\sigma^2 \eta_2}{y} \right) E' \left(\frac{\sigma^2 \eta_2}{y} \right). \quad (\text{H.1})$$

Now, we show that $\varphi(t) = (1+t)E'(t)$ is a strictly decreasing function of t . The continued fraction expansion of $E_1(t)$ is given by [33] $E'(t) = \frac{1}{t + \frac{1}{1 + \frac{1}{t+1}}}$. Ignoring high order terms, we have $E'(t) < \frac{t+1}{t(t+2)}$ for all t . Using this inequality and taking the first order derivative of $\varphi(t)$, we have $d\varphi(t)/dt = (2+t)E'(t) - 1 - 1/t < 0$. Since $\varphi(t)$ is a strictly decreasing function, the right-hand side of (H.1) is maximized by substituting $y = P_C^{\max}$, i.e., $\mathbb{E}[Z_1/Z_2] < G\mathbb{E}[Z_1]/\mathbb{E}[Z_2]$ for all (x, y) . Hence, the optimal objective of \mathcal{Q}_4 is always an upper bound on the objective of \mathcal{Q}_2 under the optimal solution. ■

APPENDIX I: COEFFICIENTS OF QUARTIC EQUATION 5

$$\begin{aligned} e_0 &= \alpha_1 a_1 K_2^2 (b_1 + 1) / \beta_1 - a_1^2 b_1 K_1 K_2 - a_1^2 b_2 K_2^2 \\ e_1 &= -2\alpha_1 a_1 b_2 K_2^2 / \beta_1 + \alpha_1 a_1 K_2 (b_1 + 1) / \beta_1 \\ &\quad + \alpha_1 a_1 b_1 K_2 / \beta_1 + 2a_1^2 b_2 K_2 (K_1 - 1) + 2a_1 a_2 b_2 K_2^2 \\ &\quad + \alpha_1 a_1 K_2 / \beta_1 + 2a_1 a_2 b_1 K_1 K_2 - 2\alpha_1 a_1 K_1 K_2 b_1 / \beta_1 \\ e_2 &= \alpha_1 a_1 b_2 K_2 (3K_1 - 4) / \beta_1 + \alpha_1 a_1 (1 + b_1 (1 - K_1)) / \beta_1 \\ &\quad + a_2 b_1 K_1 K_2 (\alpha_1 / \beta_1 - a_2) - a_1^2 b_2 (1 - K_1) \\ &\quad + a_2 b_2 K_2^2 (\alpha_1 / \beta_1 - a_2) - 4a_1 a_2 b_2 K_2 (K_1 - 1) \\ e_3 &= -2\alpha_1 a_1 b_2 (1 - K_1) / \beta_1 + 2a_1 a_2 b_2 (1 - K_1) \\ &\quad - 2a_2 b_2 K_2 (K_1 - 1) (\alpha_1 / \beta_1 - a_2) \\ e_4 &= a_2 (\alpha_1 / \beta_1 - a_2) b_2 (1 - K_1), \end{aligned}$$

with $a_1 = \sigma_D^2 + \alpha_2 / \beta_2 / \tilde{c}_{1,j}$, $a_2 = \tilde{c}_{2,j} \alpha_2 / \beta_2 / \tilde{c}_{1,j}$, $b_1 = l / \tilde{c}_{1,j}$, and $b_2 = l \tilde{c}_{2,j} / \tilde{c}_{1,j}$.

REFERENCES

- [1] A. Ramezani-Kebrya, M. Dong, B. Liang, G. Boudreau, and S. H. Seyed-mehdi, "Robust power optimization for device-to-device communication in a multi-cell network," in *Proc. IEEE ICC*, Paris, France, May 2017.
- [2] 3GPP TR 36.885 V14.0.0, Rel-14 Study on LTE-based V2X services, July 2016.
- [3] Z. Ma, M. Xiao, Y. Xiao, Z. Pang, H. V. Poor, and B. Vucetic, "High-reliability and low-latency wireless communication for Internet of Things: Challenges, fundamentals, and enabling technologies," *IEEE Internet Things J.*, vol. 6, pp. 7946–7970, Oct. 2019.
- [4] S. Kuutti, S. Fallah, K. Katsaros, M. Dianati, F. McCullough, and A. Mouzakitis, "A survey of the state-of-the-art localization techniques and their potentials for autonomous vehicle applications," *IEEE Internet Things J.*, vol. 5, pp. 829–846, Apr. 2018.
- [5] K. J. Ahmed and M. J. Lee, "Secure LTE-based V2X service," *IEEE Internet Things J.*, vol. 5, pp. 3724–3732, Oct. 2018.
- [6] L. Chen, N. Zhao, Y. Chen, F. R. Yu, and G. Wei, "Over-the-air computation for IoT networks: Computing multiple functions with antenna arrays," *IEEE Internet Things J.*, vol. 5, pp. 5296–5306, Dec. 2018.
- [7] S. Chen, J. Hu, Y. Shi, Y. Peng, J. Fang, R. Zhao, and L. Zhao, "Vehicle-to-everything (V2X) services supported by LTE-based systems and 5G," *IEEE Commun. Stand. Mag.*, vol. 1, pp. 70–76, Jul. 2017.
- [8] X. Lin, J. G. Andrews, A. Ghosh, and R. Ratasuk, "An overview of 3GPP device-to-device proximity services," *IEEE Commun. Mag.*, vol. 52, pp. 40–48, Apr. 2014.
- [9] X. Li, L. Ma, R. Shankaran, Y. Xu, and M. A. Orgun, "Joint power control and resource allocation mode selection for safety-related V2X communication," *IEEE Trans. Veh. Technol.*, vol. 68, pp. 7970–7986, Aug. 2019.
- [10] H. Yang, X. Xie, and M. Kadoch, "Intelligent resource management based on reinforcement learning for ultra-reliable and low-latency IoV communication networks," *IEEE Trans. Veh. Technol.*, vol. 68, pp. 4157–4169, May 2019.
- [11] C. Chen, B. Wang, and R. Zhang, "Interference hypergraph-based resource allocation (IHG-RA) for NOMA-integrated V2X networks," *IEEE Internet Things J.*, vol. 6, pp. 161–170, Feb. 2019.
- [12] X. Li, L. Ma, Y. Xu, and R. Shankaran, "Resource allocation for D2D-based V2X communication with imperfect CSI," *IEEE Internet Things J.*, vol. 7, pp. 3545–3558, Apr. 2020.
- [13] H. Min, W. Seo, J. Lee, S. Park, and D. Hong, "Reliability improvement using receive mode selection in the device-to-device uplink period underlying cellular networks," *IEEE Trans. Wireless Commun.*, vol. 10, pp. 413–418, Feb. 2011.
- [14] H. Min, J. Lee, S. Park, and D. Hong, "Capacity enhancement using an interference limited area for device-to-device uplink underlying cellular networks," *IEEE Trans. Wireless Commun.*, vol. 10, pp. 3995–4000, Dec. 2011.
- [15] J. Wang, D. Zhu, C. Zhao, J. Li, and M. Lei, "Resource sharing of underlying device-to-device and uplink cellular communications," *IEEE Commun. Lett.*, vol. 17, pp. 1148–1151, June 2013.
- [16] D. Feng, L. Lu, Y. Yuan-Wu, G. Y. Li, G. Feng, and S. Li, "Device-to-device communications underlying cellular networks," *IEEE Trans. Commun.*, vol. 61, pp. 3541–3551, Aug. 2013.
- [17] L. Wang and H. Wu, "Fast pairing of device-to-device link underlay for spectrum sharing with cellular users," *IEEE Commun. Lett.*, vol. 18, pp. 1803–1806, Oct. 2014.
- [18] G. Yu, L. Xu, D. Feng, R. Yin, G. Y. Li, and Y. Jiang, "Joint mode selection and resource allocation for device-to-device communications," *IEEE Trans. Commun.*, vol. 62, pp. 3814–3824, Nov. 2014.
- [19] Y. Gu, W. Saad, M. Bennis, M. Debbah, and Z. Han, "Matching theory for future wireless networks: Fundamentals and applications," *IEEE Commun. Mag.*, vol. 53, pp. 52–59, May 2015.
- [20] X. Ma, J. Liu, and H. Jiang, "Resource allocation for heterogeneous applications with device-to-device communication underlying cellular networks," *IEEE J. Sel. Areas Commun.*, vol. 34, pp. 15–26, Jan. 2016.
- [21] J. Zhao, Y. Liu, K. K. Chai, Y. Chen, and M. ElKashlan, "Joint subchannel and power allocation for NOMA enhanced D2D communications," *IEEE Trans. Commun.*, vol. 65, pp. 5081–5094, Nov. 2017.
- [22] Y. Yuan, T. Yang, H. Feng, and B. Hu, "An iterative Matching-Stackelberg game model for channel-power allocation in D2D underlaid cellular networks," *IEEE Trans. Wireless Commun.*, vol. 17, pp. 7456–7471, Aug. 2018.
- [23] R. AliHemmati, B. Liang, M. Dong, G. Boudreau, and S. H. Seyed-mehdi, "Power allocation for underlay device-to-device communication over multiple channels," *IEEE Trans. Signal Inf. Process. Netw.*, vol. 4, pp. 467–480, Sep. 2018.
- [24] —, "Multi-channel resource allocation toward ergodic rate maximization for underlay device-to-device communications," *IEEE Trans. Wireless Commun.*, vol. 17, pp. 1011–1025, Feb. 2018.
- [25] A. Ramezani-Kebrya, M. Dong, B. Liang, G. Boudreau, and S. H. Seyed-mehdi, "Optimal power allocation in device-to-device communication with SIMO uplink beamforming," in *Proc. IEEE SPAWC*, Stockholm, Sweden, June 2015, pp. 425–429.
- [26] —, "Joint power optimization for device-to-device communication in cellular networks with interference control," *IEEE Trans. Wireless Commun.*, vol. 16, pp. 5131–5146, Aug. 2017.
- [27] A. Abu Al Haija and M. Vu, "Spectral efficiency and outage performance for hybrid D2D-infrastructure uplink cooperation," *IEEE Trans. Wireless Commun.*, vol. 14, pp. 1183–1198, Mar. 2015.
- [28] D. Feng, L. Lu, Y. W. Yi, G. Y. Li, G. Feng, and S. Li, "QoS-aware resource allocation for device-to-device communications with channel uncertainty," *IEEE Trans. Veh. Technol.*, vol. 65, pp. 6051–6062, Aug. 2016.
- [29] A. Memmi, Z. Rezk, and M. S. Alouini, "Power control for D2D underlay cellular networks with channel uncertainty," *IEEE Trans. Wireless Commun.*, vol. 16, pp. 1330–1343, Feb. 2017.
- [30] B. V. R. Gorantla and N. B. Mehta, "Resource and computationally efficient subchannel allocation for D2D in multi-cell scenarios with partial and asymmetric CSI," *IEEE Trans. Wireless Commun.*, vol. 18, pp. 5806–5817, Dec. 2019.
- [31] T. Zahir, K. Arshad, A. Nakata, and K. Moessner, "Interference management in femtocells," *IEEE Commun. Surveys Tuts.*, vol. 15, pp. 293–311, 2013.
- [32] A. Ramezani-Kebrya, I.-M. Kim, F. Chan, R. Inkol, and H.-K. Song, "Detection for an AF cooperative diversity network in the presence of interference," *IEEE Commun. Lett.*, vol. 17, pp. 653–656, Apr. 2013.
- [33] M. Abramovitz and I. A. Stegun, *Handbook of Mathematical Functions with Formulas, Graphs, and Mathematical Tables*. New York, USA: Dover, 1972.
- [34] H. Kuhn, "The Hungarian method for the assignment problem," *Nav. Res. Logist. Quart.*, vol. 2, pp. 83–97, Mar. 1955.
- [35] D. Gale and L. S. Shapley, "College admissions and the stability of marriage," *American Math. Monthly.*, vol. 69, pp. 9–15, Jan. 1962.
- [36] I. S. Gradshteyn and I. M. Ryzhik, *Table of Integrals, Series, and Products*. Elsevier, 2007.



Ali Ramezani-Kebrya (Member, IEEE) received the B.Sc. degree from the University of Tehran, Tehran, Iran, the M.A.Sc. degree from Queen's University, Kingston, Canada, and the Ph.D. degree from the University of Toronto, Toronto, Canada. From 2018 to 2021, he was a Postdoctoral Fellow at the Vector Institute, Toronto, Canada. In 2021, he joined the Laboratory for Information and Inference Systems at EPFL, Lausanne, Switzerland, where he is currently a Senior Scientific Collaborator. His current research interests are in machine learning, reinforcement learning, privacy/security, optimization, and communications/networking. He received the Natural Sciences and Engineering Research Council of Canada Postdoctoral Fellowship.



Ben Liang (Fellow, IEEE) received honors-simultaneous B.Sc. (valedictorian) and M.Sc. degrees in Electrical Engineering from Polytechnic University (now the engineering school of New York University) in 1997 and the Ph.D. degree in Electrical Engineering with a minor in Computer Science from Cornell University in 2001. He was a visiting lecturer and post-doctoral research associate at Cornell University in the 2001 - 2002 academic year. He joined the Department of Electrical and Computer Engineering at the University of Toronto

in 2002, where he is now Professor and L. Lau Chair in Electrical and Computer Engineering. His current research interests are in networked systems and mobile communications. He is an associate editor for the IEEE Transactions on Mobile Computing and has served on the editorial boards of the IEEE Transactions on Communications, the IEEE Transactions on Wireless Communications, and the Wiley Security and Communication Networks. He regularly serves on the organizational and technical committees of a number of conferences. He is a Fellow of IEEE and a member of ACM and Tau Beta Pi.



Min Dong (Senior Member, IEEE) received the B.Eng. degree from Tsinghua University, Beijing, China, in 1998, and the Ph.D. degree in electrical and computer engineering with a minor in applied mathematics from Cornell University, Ithaca, NY, in 2004. From 2004 to 2008, she was with Qualcomm Research, Qualcomm Inc., San Diego, CA. Since 2008, she has been with Ontario Tech University, where she is currently a Professor with the Department of Electrical, Computer and Software Engineering and the Associate Dean (Academic) of the

Faculty of Engineering and Applied Science. Her research interests include wireless communications, statistical signal processing, learning techniques, optimization and control applications in cyber-physical systems.

Dr. Dong received the Early Researcher Award from the Ontario Ministry of Research and Innovation in 2012, the Best Paper Award at IEEE ICC in 2012, and the 2004 IEEE Signal Processing Society Best Paper Award. She is a co-author of Best Student Paper of Signal Processing for Communications and Networking at IEEE ICASSP 2016. She currently serves on the Steering Committee of the IEEE TRANSACTIONS ON MOBILE COMPUTING. She is an Editor for the IEEE TRANSACTIONS ON WIRELESS COMMUNICATIONS. She served as an Associate Editor for the IEEE TRANSACTIONS ON SIGNAL PROCESSING (2010-2014), and as an Associate Editor for the IEEE SIGNAL PROCESSING LETTERS (2009-2013). She was an elected member of the Signal Processing for Communications and Networking (SPCOM) Technical Committee of IEEE Signal Processing Society (2013-2018). She was the lead Co-Chair of the Communications and Networks to Enable the Smart Grid Symposium at the IEEE International Conference on Smart Grid Communications in 2014.



Gary Boudreau (Senior Member, IEEE) received a B.A.Sc. in Electrical Engineering from the University of Ottawa in 1983, an M.A.Sc. in Electrical Engineering from Queens University in 1984 and a Ph.D. in electrical engineering from Carleton University in 1989. From 1984 to 1989 he was employed as a communications systems engineer with Canadian Astronautics Limited and from 1990 to 1993 he worked as a satellite systems engineer for MPR Teltech Ltd. For the period spanning 1993 to 2009 he was employed by Nortel Networks in a

variety of wireless systems and management roles within the CDMA and LTE basestation product groups. In 2010 he joined Ericsson Canada where he is currently employed in the 5G systems architecture group. His interests include digital and wireless communications as well as digital signal processing.